Title

COHERENT X RAYS AND VACUUM-ULTRAVIOLET RADIATION FROM STORAGE-RING-BASED UNDULATORS AND FREE ELECTRON LASERS

Author

Kim, K-J.

Publication Date

1984-12-01

LBL-18945
c.2

Coherent X Rays and Vacuum-Ultraviolet Radiation from Storage-Ring-Based Undulators and Free Electron Lasers

December 1984

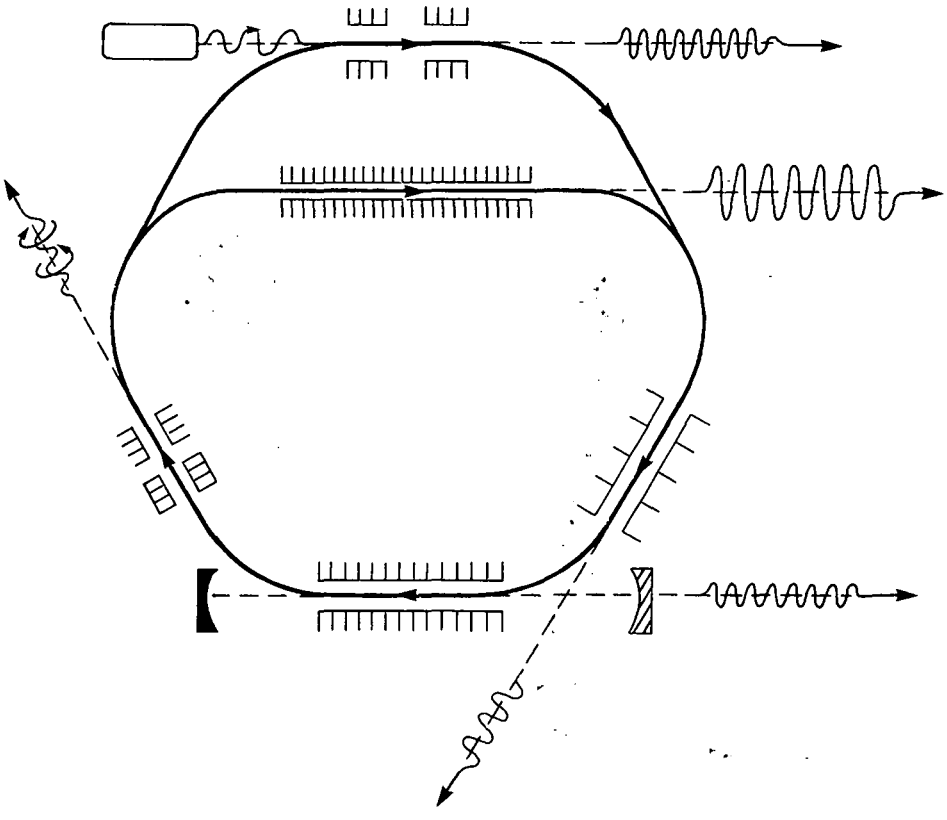

Lawrence Berkeley Laboratory
University of California
Berkeley, California 94720

Prepared for the U.S. Department of Energy under Contract DE-AC03-76SF00098

DISCLAIMER

LBL-18945

COHERENT X RAYS AND VACUUM-ULTRAVIOLET RADIATION FROM STORAGE-RING-BASED UNDULATORS AND FREE ELECTRON LASERS

Kwang-Je Kim, Editor

Center for X-Ray Optics
Lawrence Berkeley Laboratory
University of California
Berkeley, California 94720

This work was supported by the U.S. Department of Energy
under Contract No. DE-AC03-76SF00098.

Summary

High-brightness electron storage rings and permanent-magnet technology provide a basis for the development of coherent radiation in the 10- to 1000-Å (XUV) spectral range. The most assured route to the production of coherent x rays and VUV is the simple interaction between properly constrained relativistic electrons and permanent-magnet undulators, a subject that is already well understood and where technology is well advanced. Other techniques are less well developed, but with increasing degrees of technical challenge they will provide additional coherence properties.

Transverse optical klystrons (TOKs) provide an opportunity for additional coherence at certain harmonics of longer-wavelength lasers. Free electron lasers (FELs) extend coherence capabilities substantially through two possible routes: one is the development of a high-gain, single-pass lasing system; the second is based on formation of an x-ray optical cavity (laser cavity) through the development of suitable mirror coatings. Both FEL techniques would provide VUV radiation and soft x rays with extremely narrow spectral content. Research on all of these techniques (undulators, TOKs, and FELs) is possible in a single facility based on a high-brightness electron storage ring, referred to herein as a Coherent XUV Facility (CXF).

Preface

This report was conceived during two international conferences on FELs held in Italy on September 5 and September 15, 1984. As an outcome of those conferences, a position paper on the timeliness of a short-wavelength FEL facility was proposed. This report is in response to that proposal. Each author has contributed a section within his own area of expertise. The report is a collection of contributions by the individual authors, who agree that such a facility is now required for further advancement in the development of coherent XUV sources.

CONTENTS

1. Introduction--A Short-Wavelength-FEL/Storage-Ring Complex

Andrew M. Sessler
Lawrence Berkeley Laboratory

Remarkable progress has been made, during the last two years, on free electron lasers (FELs). After the first FEL was made to work by Madey et al., there was a five-year hiatus in experimental results. During this time there was a great deal of theoretical work, but the theory was far ahead of (and consequently often irrelevant to) the experimental programs.

Recently FELs have been operated at MSNW, TRW (at Stanford), LANL, LBL/LLNL, MIT, NRL, Columbia (at NRL), the Lebedev Institute, Orsay, and UC Santa Barbara. There are experimental programs that have not yet made operational FELs at Frascati (2 groups), Novosibirsk, BNL, and Glasgow. The construction and operation of FELs have now reached a new level; there is no longer any doubt that FELs can be made to operate. Furthermore, there is now considerable understanding of, and a wealth of experience with, FELs, so that the performance of a proposed FEL facility can be predicted with confidence. In addition, the time is ripe for pushing the operating parameters into new regions.

In particular, we believe that, in view of the present state of FEL understanding, it is now proper to construct a research facility devoted to the use of coherent radiation and the advancement of FEL physics technology at wavelengths shorter than 1000 Å. In Fig.1-1, we show a possible layout of such a facility, which will be referred to as a Coherent XUV Facility (CXF), where research can be conducted on several techniques for generating coherent radiation. Undulators are already well understood and will generate broadly tunable, spatially coherent radiation of bandwidth $\lambda/\Delta\lambda \approx 10^2$. A crossed undulator system will extend the undulator capability to include variable polarization. For full coherence, in spatial as well as in longitudinal directions, it is necessary to induce and exploit density modulation in electron beams, as is the case in the transverse optical klystrons (TOKs) and FELs. In TOKs, coherent radiation is generated at harmonics of an input laser frequency, with the electron beam playing the role of a nonlinear medium. Ultimately, FELs would deliver intense, tunable x rays and VUV radiation of extremely narrow spectral width. There are two possible routes to an FEL, one based on feedback by end mirrors, the other based on development of a high-gain, single-pass device.

It can readily be seen, from of the remaining sections of this paper, that the photon flux increases monotonically, or the wavelength decreases monotonically, as one goes through (1) undulator radiation, (2) TOK radiation, (3) FEL oscillator radiation, to (4) FEL single-pass radiation. Each of these will demand considerable quality development effort. Each will result in photon fluxes of increased value to the users. Such radiation should, and will be, used. It is

important, however, to restrict the usage so that adequate time (perhaps ≃ 50% of the time) is available for further advancement of the FEL technology. In short, it is proposed that the FEL/Storage-Ring facility will both advance FEL physics and produce interesting fluxes of coherent photons.

Central to the above techniques are electron storage-ring technology and magnetic-undulator technology. An electron storage ring suitable for FEL application should be able store 500-1000 MeV electron beams of low emittance (~ 10^{-8} πm-rad), high peak current (~ 200 A), and low energy spread ($\Delta E/E$ ~ 0.001). Long undulators (N ~ 100-1000) with short periods (λ_u ~ few cm) have been designed using permanent-magnet technologies. The tolerance on field quality are tight, especially for TOK and FEL applications.

Such a facility will not be inexpensive, perhaps costing tens of millions of dollars. On the other hand, approximately 40 million dollars per year is being spent, in the U.S., on FELs. Civilian expenditures are roughly $4M/year, so that the proposed facility will require a step function in non-military spending, perhaps by a factor of three.

In Section 2, we review characteristics of undulator radiation including spatial and longitudinal coherence properties, comparison of coherent power from undulators and laser harmonics techniques, polarization control, etc. In Section 3, we consider harmonic generation of coherent radiation using a TOK. A TOK has been successfully operated at Orsay, starting at 1 μm (Nd: glass laser). Similar work is now being undertaken by the Bell Labs/BNL group at the VUV ring of NSLS. Of course, the TOK proposed would start at a much shorter wavelength driven, for example, by an excimer laser.

In Section 4, we discuss an FEL oscillator similar to that which has been operated, at Orsay, in the visible spectrum. Extension of this technology, to shorter and shorter wavelengths, depends most crucially on the development of "good" mirrors, i.e., non-degradable mirrors with significant normal incidence reflectivity. Mirrors with 50% reflectivity are theoretically possible down to 400 Å and thus may provide the basis for a short-wavelength FEL oscillator, as discussed in Section 4.

In Sections 5 and 6, we consider the generation of coherent radiation by a single-pass super-radiant FEL, referred to as Self-Amplified Spontaneous Emission (SASE) in Section 6. This is the analog, now in the soft-x-ray range, of the LBL/LLNL experiment in the microwave range (Section 5). For this approach we need no mirrors; the radiation simply grows, in a single pass, from noise. Important to the operation of this FEL is the optical guiding of light, since the wiggler will be many Rayleigh lengths long.

The physics of a low-emittance, high-current storage ring is discussed in Sections 7 and 8. Basic concepts of lattice design are presented in Section 7. Finally in Section 8, we discuss the impact of coherent and incoherent multiparticle phenomena on storage-ring design.

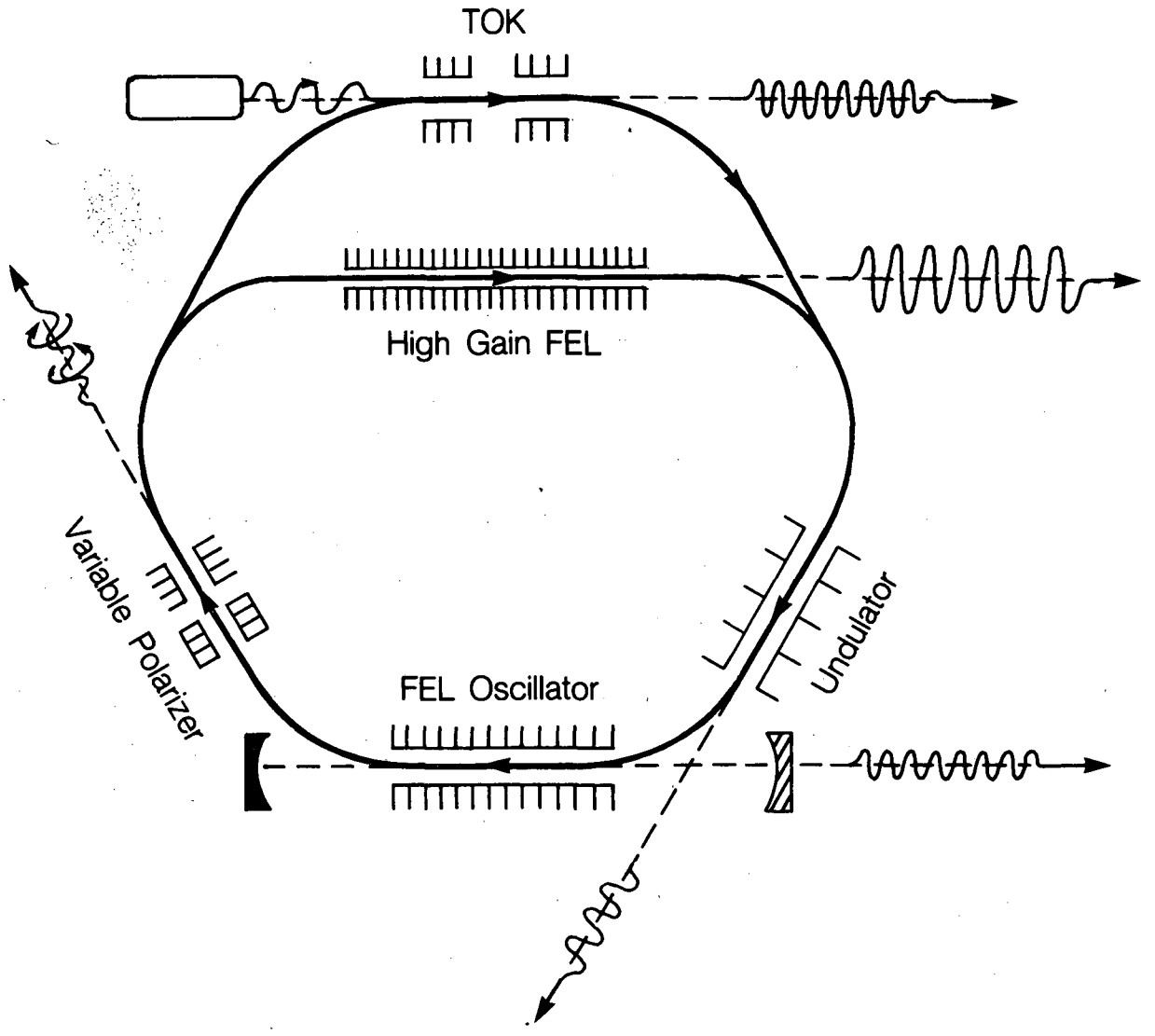

Figure 1-1. Conceptual layout of a coherent XUV facility.

2. Coherent VUV Radiation and Soft X Rays from Undulators in Modern Storage Rings*

Kwang-Je Kim, Klaus Halbach, and David Attwood
Lawrence Berkeley Laboratory

Magnetic structures in modern storage rings provide an assured route to fundamentally new opportunities for extending coherent radiation experiments to the vacuum-ultraviolet and soft-x-ray spectral regions. Coherent power levels of about 10 mW are anticipated, in a fully spatially coherent beam, with a longitudinal coherence length of about 1 μm. In addition to broad tunability and polarization control, the radiation would occur in 20-psec pulses, at a 500-MHz repetition rate.

Undulators in modern storage rings are capable of generating substantial coherent power in the heretofore inaccessible spectral region extending from photon energies of a few eV to several thousand eV. In addition to providing an assured route to coherent techniques in the important soft-x-ray and vacuum-ultraviolet spectral regions (collectively referred to here as the XUV), the radiation is also broadly tunable. The latter feature is a significant advantage with respect to x-ray lasers that might become available in the next decade or so in that it permits imaging and spectroscopic probe studies to be conducted around the important atomic and molecular resonances so prominent in that region. In this section we give an introductory review of the coherence characteristics of undulator radiation.

2.1 Modern Synchrotron Radiation Sources

An extremely relativistic electron experiencing bending motion produces a narrow cone of synchrotron radiation in the direction of its instantaneous motion.[2-1] The angular width of the radiation cone, γ^{-1}, is typically several hundred microradians, where γ is the ratio of total electron energy to its rest energy.

Historically, the primary source of synchrotron radiation in storage rings has been at the bending magnets, as illustrated at the top of Fig. 2-1. However, bending-magnet radiation is incoherent and is spread across a wide horizontal fan. A more efficient way of producing and collecting synchrotron radiation involves use of periodic magnet structures, in particular, permanent magnets that permit combination of high field strengths with short periods.[2-2] This general scheme is illustrated in Figs. 2-1 and 2-2. These many-period magnetic structures produce an N-fold increase in radiated flux, where N is the number of periods, and they offer options for spectrally shifting to higher photon energies with a strong-field "wiggler" or coherent intensification on axis with a moderate-field "undulator." The parameter determining this option is the deflection parameter

*An updated version of this paper will be published in a forthcoming issue of Science (1985).

K = 0.934 times peak magnetic field strength in tesla times period length in cm. K is the ratio of the maximum electron deflection angle to the natural radiation angle, γ^{-1}. For $K \gg 1$, the wiggler case, the electron experiences large magnetic deflections, thus producing more flux at higher photon energies and radiating into a proportionately larger radiation cone. Although the radiation they produce is incoherent, wigglers are currently the most powerful sources of laboratory x rays.[2-3]

Undulators, for which $K \lesssim 1$, are fundamentally different. The radiated fields associated with various magnetic periods all fall within the primary radiation cone of the individual relativistic electrons. Consequently, interference effects occur between radiation from the various periods. This results in N-fold field additions on axis, or N^2 increases of power density (intensity) on axis. To the present synchrotron radiation community, this would be described as a greater source "brightness." More significantly, undulators have introduced substantial coherent radiation opportunities to important regions of the spectrum.

2.2 Coherent Undulator Radiation

The spectral characteristics of undulator radiation can be understood by considering the radiation seen by an observer fixed in the laboratory frame, looking directly at the relativistic electron as it passes through the magnetic structure. Electromagnetic waves, emitted as the electron passes successive periods of the structure, will arrive at the fixed observer at times separated by $\Delta t = \lambda_u (1-\beta_z)/c$, where λ_u is the magnetic period length, c is the velocity of light in vacuum, and $c\beta_z$ is the electron's average velocity in the z-direction. In the extreme relativistic case, $\beta_z = 1 - (1 + K^2/2)/2\gamma^2$, from which it follows that the radiated fields are relativistically contracted from the undulator period λ_u to an electromgnetic wavelength

$$\lambda_x = c\Delta t = \frac{\lambda_u(1 + K^2/2)}{2\gamma^2} \qquad (2\text{-}1)$$

and its harmonics, λ_x/n. Since γ is large (~1,000), undulator periods on the order of 1 cm are contracted to soft-x-ray wavelengths on the order of 100 Å, with shorter-wavelength harmonics. Changing the magnet gap changes the peak field B_0, providing easily tuned radiation (through variations in K).

To realize the benefits of a coherent undulator, it is necessary that the electron beam be sufficiently constrained in phase space to ensure that these interference effects are not washed out. That is, the electron beam must be constrained to an area solid-angle product comparable to a diffraction-limited phase space at the desired wavelength. When this condition is achieved the entire radiated flux will be spatially coherent within a certain coherence length.[2-4]

The technological breakthrough permitting this extension of coherent radiation techniques to the XUV has been provided by the accelerator design community, which can now construct a storage ring whose electron beam is characterized by a (space-angle phase-space) "emittance" comparable to that of the diffraction-limited radiation source of 100-Å wavelength. Quantitatively, the resulting radiation will be spatially coherent if the phase space of the electron beam, described by the horizontal and vertical emittances ε_x and ε_y, is equal to or less than the diffraction-limited radiation phase space defined by $d(2\theta) = 2.4\lambda_x$, where λ_x is the wavelength. When this condition prevails, that is, when

$$\varepsilon_x \varepsilon_y < (2.4\lambda_x)^2 \qquad (2\text{-}2)$$

the resulting radiation will be spatially coherent.

Throughout this section, the quantitative characteristics of future undulator sources will be described in terms of a fully designed and optimized facility, LBL's proposed Advanced Light Source (ALS).[2-5] A CXF operating at 1.3 GeV will give similar, although somewhat lower, performance because it is optimized for FEL operation at a lower energy (750 MeV). The spatial radiation pattern of an undulator designed for ALS is shown in Fig. 2-3.

Undulator radiation is both spatially and longitudinally coherent, displaying spectral peaks of width $\lambda_x/\Delta\lambda_x \sim N$, as illustrated in Fig. 2-4. The coherence length, for interference of mismatched experimental path lengths, is defined as $\ell_c = \lambda_x^2/\Delta\lambda_x = N\lambda_x$. For a 100-period undulator radiating at a fundamental of 100 Å, this would give a 1-μm coherence length, sufficient, for instance, for many anticipated soft-x-ray microprobe and microholograph experiments. Where longer coherence lengths are required, or where greater spectroscopic purity is required, one can introduce monochromators for order-of-magnitude improvements, with proportionate losses of power. The issues of partial and longitudinal coherence are summarized in Fig. 2-5.

To the extent that the above two criteria for spatial and longitudinal coherence are satisfied, all photons produced by the undulator/electron-beam interaction are fully capable of mutual interference. At optimum or longer wavelengths, the coherent volume is set by, and fully includes, the full spatial extent of the electron beam, through a coherence length set by the relativistically contracted length of the undulator. For shorter-wavelength radiation, shorter than determined by equivalent electron and photon phase spaces, aperturing must be employed to assure full spatial coherence. For the ALS undulator D, designed for third-harmonic radiation at 500 eV (25 Å), moderate aperturing and monochromatization results in fully coherent soft-x-ray radiation at an average power level of 10 mW, with a coherence length of several micrometers. The radiation will be tunable over a broad spectral range that includes the K-edges of such important elements as carbon, oxygen, and nitrogen. Further,

the radiation will occur in 20-psec pulses at a 500-MHz repetition rate.[2-6] Similar performance will be available in the VUV, using separate undulators specifically designed for that wavelength range and placed elsewhere in the ring. The proposed ALS has twelve long straight sections to accommodate different undulators optimized for use in different spectral ranges. The projected ALS capabilities are summarized in Fig. 2-6 for four of its undulators (A, B, C, and D).

For comparative purposes, Fig. 2-6 also shows the results of recent nonlinear laser harmonic and mixing experiments.[2-7] Producing radiation in 10-psec to several-nsec bursts, typically at 10-Hz repetition rates, these radiation sources fall off very rapidly in power at photon energies beyond 10 eV, typically as wavelength to an exponent about equal to the nonlinearity involved, e.g., λ^9.

In addition, we note that, if available, true lasers would be characterized by narrower spectral content and higher peak power, thus complementing tunable coherent undulator radiation capabilities as described here. At the present, however, high-reflectivity mirrors do not exist for the XUV, although progress in their development is being made.[2-8] If such optics did become available, the undulator/storage-ring techniques described here could be operated as XUV free electron lasers (FELs), also broadly tunable but of greatly increased spectral purity and power. Other proposed schemes for (soft) x-ray lasing are likely to be of high spectral purity, will perhaps involve a few discrete spectral lines, but will not be broadly tunable across absorption features of interest to the experimenter. In addition, such potential lasing schemes would likely be single-pass super-radiant schemes, also quasi-coherent in nature. They are also likely to be driven, at least in their early stages, by large pulsed-energy facilities, for example, high-power lasers originally developed for inertial fusion.

2.3 Polarization Control

In addition to the space-time characteristics of electromagnetic radiation, there is also polarization. In this section we describe a method[2-9] that uses a sequential pair of crossed undulators to obtain complete polarization control. The concept is illustrated in Fig. 2-7. Each undulator produces radiation on the axis of linear polarization. By properly overlapping the two cross-polarized wave trains, it is possible to produce linear or circular polarization, depending on their relative phases. Phase variation in this scheme is controlled by an electron path modulator between the two linear undulators--effectively using modulated electron transit time to the second undulator as a means of varying phase between the two wave trains--each of which is driven by the electron beam. To maintain well-defined polarization and phase control, it is again necessary that the electron beam emittance be small. Variable polarization control is expected to play an important role in future experiments, such as in probes of biochemical structures in which image contrast or differential scattering signals are provided by polarization-sensitive

scattering from structures in which the diameter or helical pitch may be of sizes comparable to the probing VUV or soft-x-ray wavelength. Table 2-1 summarizes parameters that characterize variable polarization capabilities that could be provided at two potential sites, BNL's present VUV ring and LBL's proposed ALS.

2.4 Conclusion

Coherent VUV and soft-x-ray radiation is predictably available with modern low-emittance storage rings and permanent-magnet undulators. While covering a wide spectral region and producing broadly tunable radiation, these facilities will provide pulses typically of 20-psec duration at a 500-MHz repetition rate. In Table 2-2, we have summarized typical parameters for a soft-x-ray undulator.

2.5 References

2-1. H. Winick and S. Doniach, Synchrotron Radiation Research (Plenum Press, New York, 1980).

2-2. K. Halbach, Nucl. Instrum. Methods 187 109 (1981); J. Phys. Colloque C1 - 211, Tome 44 (1983).

2-3. E. Hoyer et al., Nucl. Instrum. Methods 208, 117 (1983).

2-4. The coherence properties of synchrotron radiation were first described by A.M. Krondratenko and A.N. Skrinsky [Opt. Spectrosc. 42, 189 (1977)] using intuitive arguments. A rigorous description of undulator coherence properties in terms of correlated field quantities is to be given in a forthcoming paper by K.-J. Kim.

2-5. Advanced Light Source Conceptual Design Report, Lawrence Berkeley Laboratory, Berkeley, CA, PUB-5084 (1983); see also R.C. Sah, IEEE Trans. Nucl. Sci. NS-30, 3100 (1983).

2-6. R.C. Sah, A.P. Sabersky, and D.T. Attwood, "Picosecond Pulses for Future Synchrotron Radiation Sources," submitted to Topical Meeting on Ultrafast Phenomena, Monterey, CA, June 1984.

2-7. See papers presented at the American Institute of Physics Topical Meeting on Laser Techniques in the Extreme Ultraviolet, Boulder, CO, March 5-7, 1984.

2-8. D.T. Attwood et al., "Report of the Working Group on Short Wavelength Optics," Proceedings of the Conference on Free Electron Generation of Extreme Ultraviolet Coherent Radiation, Brookhaven, September 1984, J.M.J. Madey and C. Pellegrini, Eds. (Optical Society of America, 1983).

2-9. K.-J. Kim, "A Synchrotron Radiation Source with Arbitrarily Adjustable Elliptical Polarization," New Rings Workshop, SSRL Report, Stanford, CA (1983); also Nucl. Instrum. Methods 219, 425 (1984).

Table 2-1. Two potential sources of variable polarization radiation.

	VUV (NSLS)	ALS
E_θ	750 MeV	1.3 GeV
σ_θ	9×10^{-2} mrad	2×10^{-2} mrad
N	5	30
λ_u	10 cm	4 cm
λ_1 (ϵ_1)	470 Å (26 eV)	47 Å (260 eV)
$\Delta\lambda/\lambda$	4%	0.14%
Flux at Sample (1% Optical Efficiency)	$\sim 10^{12}$ photons/sec	$\sim 10^{12}$ photons/sec

Table 2-2. Typical parameters for a soft-x-ray undulator.

Electron Beam Energy	1 GeV ($\gamma = \frac{E}{m_0 c^2} = 2{,}000$)
Beam Current	0.4 A
Magnetic Wavelength (λ_u)	3 cm
Magnetic Periods (N)	100
Photon Wavelength (λ_x)	$\frac{\lambda_u}{2\gamma^2} = 25$ Å (500 eV) (Broadly tunable, 100 eV to few keV)
Bandwidth ($\frac{\lambda_x}{\Delta\lambda_x}$)	N = 100
Angular Width (2θ)	$\frac{1}{\gamma\sqrt{N}} \sim 50$ μrad
Polarization	Linear, circular, ...
Radiated Power	1 W cw in 20-psec bursts
Coherent Power	10 mW at 500 eV, tunable (spatially coherent, $\ell_c = \frac{\lambda^2}{\Delta\lambda} \sim N\lambda$ few μm)

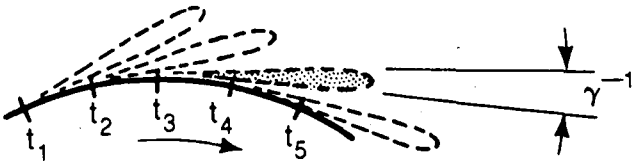

Bending Magnet — A "Sweeping Searchlight"

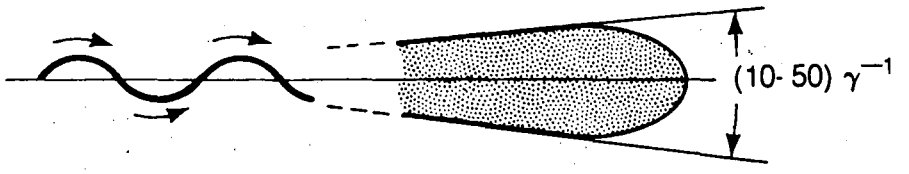

Wiggler — Incoherent Superposition

$$\frac{dP}{d\Omega} \propto N$$

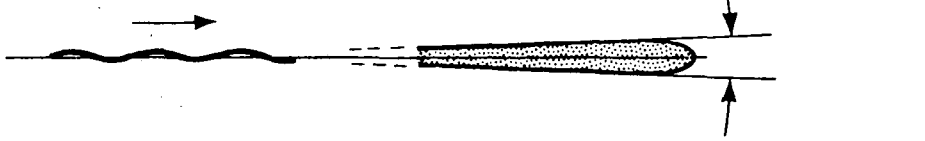

Undulator—Coherent Interference

$$\frac{dP}{d\Omega} \propto N^2$$

$$\Omega \propto \frac{1}{N}$$

$$P \propto N$$

N = number of magnetic periods (~100)

$$\gamma^{-1} = \frac{m_o c^2}{E_e} = \frac{0.511}{E_e(\text{GeV})} \text{ mrad}$$

XBL 8311-4541

Figure 2-1. Synchrotron radiation sources include (a) historically significant bending magnets, with relativistically narrowed radiation patterns, (b) multiperiod strong-field wigglers, and (c) many-period coherent undulators.

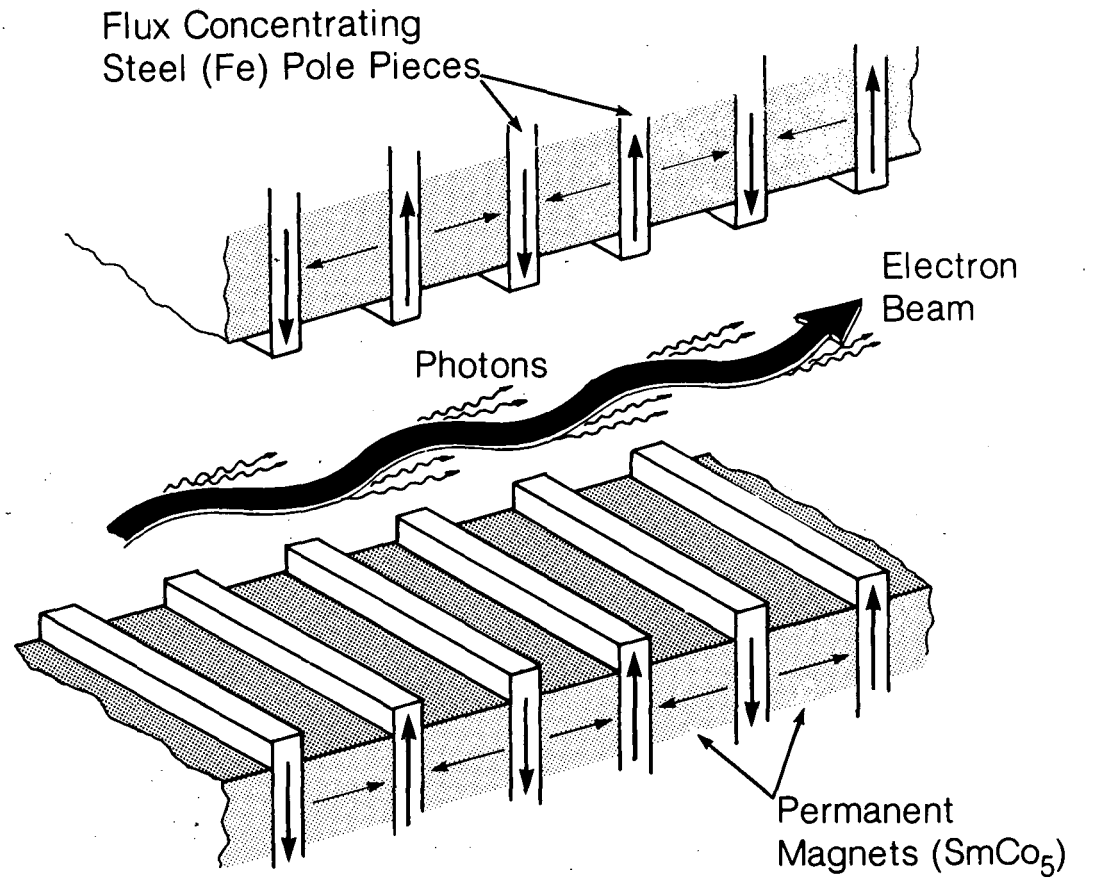

Figure 2-2. Many-period magnetic insertion devices generate an N-fold increase in radiated power. Wigglers are strong-field structures, driving electron trajectories of large angles, leading to an incoherent superposition of fields. Undulators employ electron deflections within the nominal radiation cone, such that a coherent superposition of fields dominates. The result is on-axis field intensification, radiation cone narrowing, and substantial coherence properties in modern low-emittance storage rings.

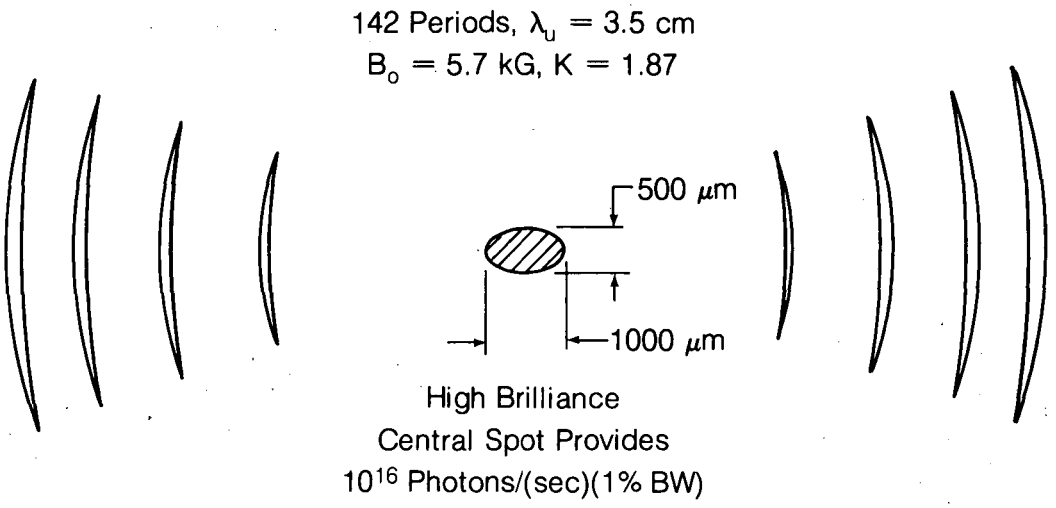

Figure 2-3. The spatial distribution of undulator radiation, demonstrating coherent interference at 500-eV photon energy. Calculations are for undulator D of the proposed ALS synchrotron facility at LBL (Ref. 2-5).

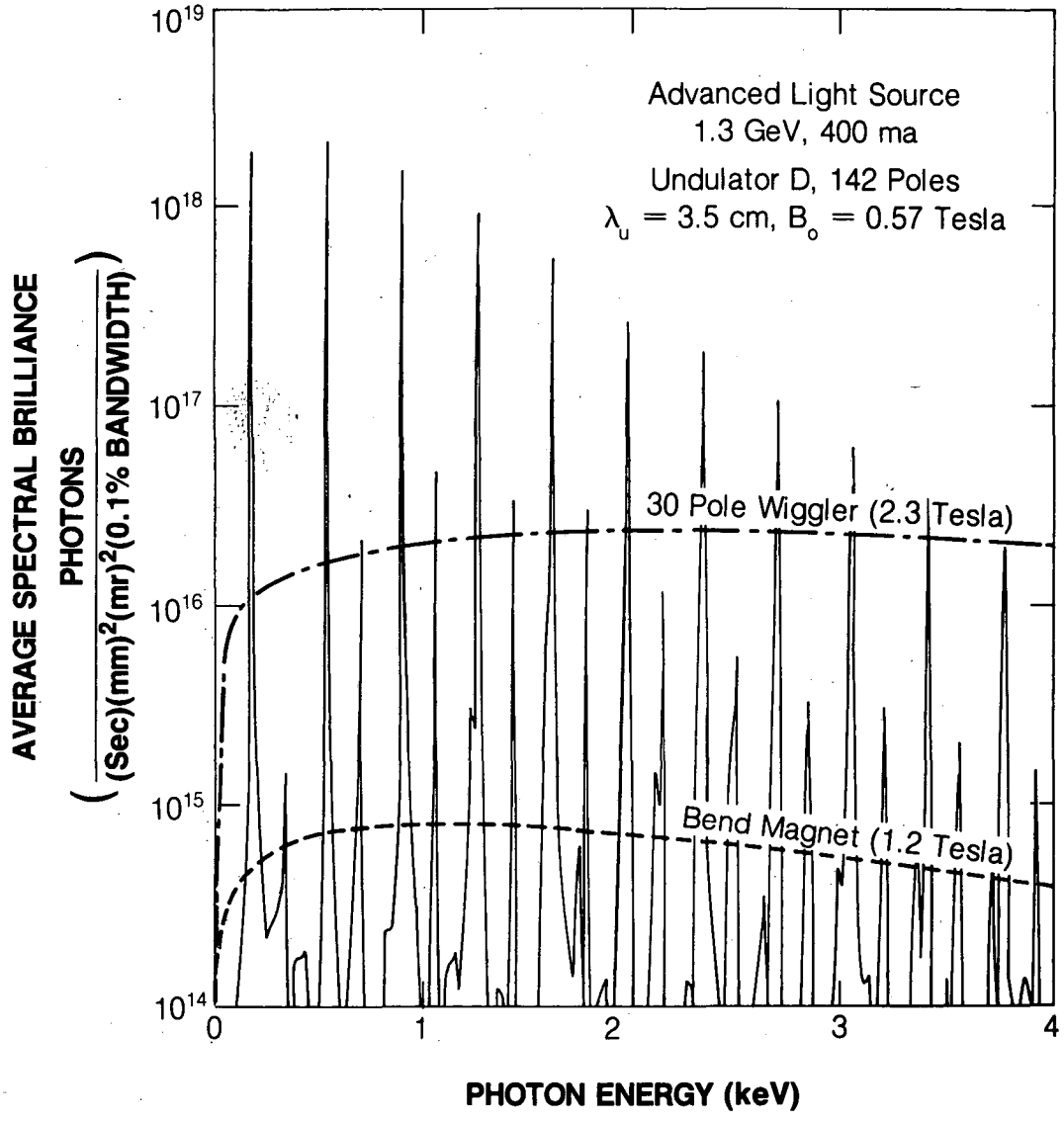

Fig. 2-4. Spectral characteristics (harmonic structure) of undulator D radiation, compared with that of a wiggler and a bending magnet at the ALS.

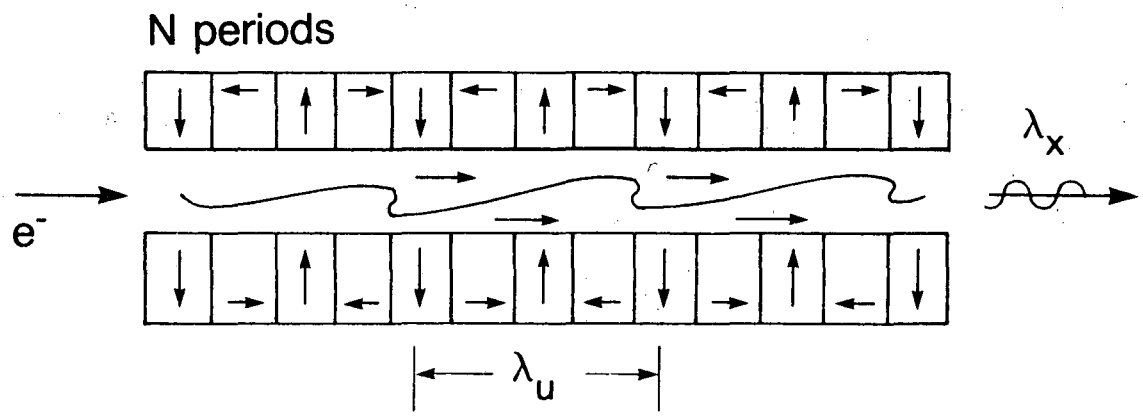

XBL 842-9418 B

Figure 2-5. Quasi-coherent soft x rays are produced in a straightforward manner via the interaction of a well-controlled low-emittance relativistic electron beam and a high-fidelity magnetic undulator. Relativistic contraction gives a radiation wavelength $\lambda_X = \lambda_U/2\gamma^2$. Further, the relativistically narrowed cone and small beam size (phase space, $\Delta A \cdot \Delta\Omega$) lead to near-diffraction-limited (spatially coherent) soft x rays. The longitudinal "coherence length" is given by $\ell_C = \lambda_X^2/\Delta\lambda_X = N\lambda_X$.

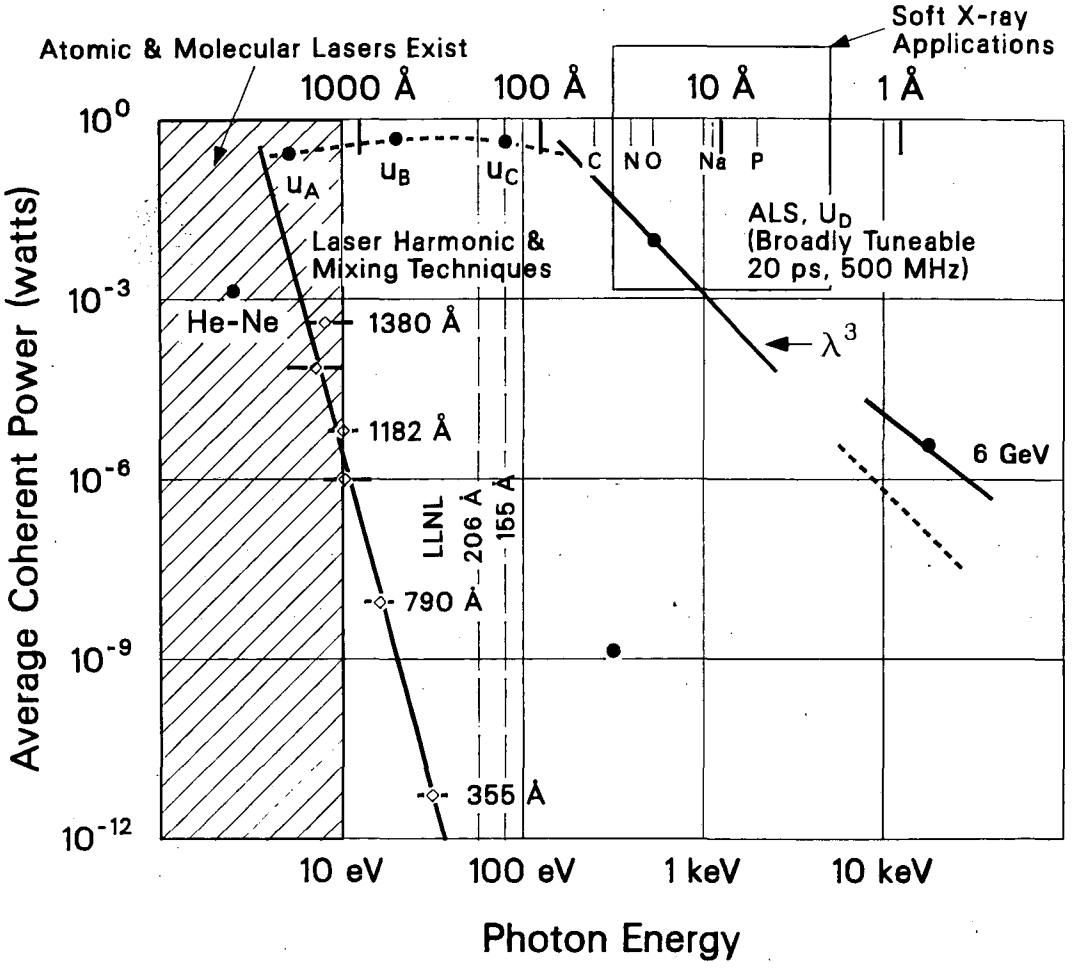

*Full spatial coherence; longitudinal coherence ≧ 1μm

XCG 843-13016 D

Figure 2.6. Broadly tunable coherent radiation will be available--via an assured route--at interesting power levels throughout the VUV and soft-x-ray spectral ranges. Laser harmonic and mixing techniques are not competitive in the region beyond 10 eV. Potential XUV lasers may ultimately provide narrower spectral features and higher peak powers but will not likely provide broad tunability and thus are complementary to coherent undulator techniques. Undulators may also provide additional capabilities as bunching techniques and mirrors (FELs) become available.

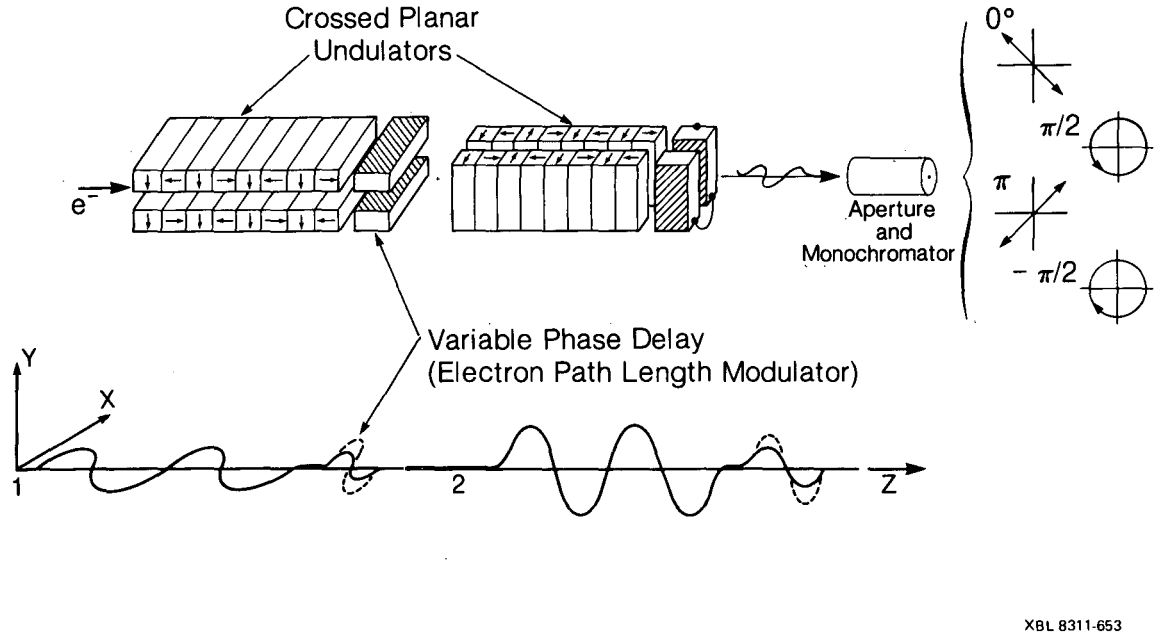

Figure 2.7. Variably polarized radiation can be generated by using crossed undulators in low-emittance storage rings.

3. Production of Coherent XUV and Soft-X-Ray Light Using a Transverse Optical Klystron

Brian M. Kincaid and Richard R. Freeman
AT&T Bell Laboratories

This section describes the theory of the production of coherent XUV radiation and soft x rays using a transverse optical klystron (TOK). A TOK uses a high-power laser in conjunction with an undulator magnet to produce laserlike output of XUV radiation from a relativistic electron beam.

With the recent demonstration of a storage-ring-based free electron laser (FEL) operating in the visible spectrum, the future of FEL sources of coherent radiation appears particularly auspicious. The advances in FEL physics will be substantial in the demonstration of FEL oscillation in the near UV; meanwhile, however, there is an immediate need in the laser/spectroscopy community for a tunable laser source between 500 and 2000 Å. In this region, no laboratory source of widely tunable, high-power coherent radiation is currently available. Using the TOK harmonic technique, it should be possible to reach this wavelength and beyond using presently available storage rings. Since the TOK does not use an optical cavity but rather uses the electrons in the storage ring as a kind of nonlinear optical medium, operation is not limited by mirror losses, as in the FEL. As a result, the TOK does not produce a high average power, though it can provide a useful ($\sim 10^{-3}$ to 10^{-6}) conversion of the input laser peak power to harmonic output.

An optical klystron is a device in which a relativistic electron beam produces coherent electromagnetic radiation by interacting with an external laser beam in an undulator magnetic field. This device is the relativistic generalization of the microwave klystron.[3-1] Because the energy exchange between the electrons and the light is, in this case, due to the transverse electric field of the laser, the device is called a transverse optical klystron. As in an ordinary klystron, coherent radiation is produced at the harmonics as well as at the fundamental of the input laser frequency, resulting in a relatively efficient conversion of the input visible laser to output wavelengths in the extreme ultraviolet.

The generation of coherent light by the TOK can be described as a three-step process: energy modulation, compaction or bunching, and radiation. A schematic representation of the TOK is shown in Fig. 3-1. In the first section, the electron beam is energy modulated by the combined action of the laser and the undulator magnet. The energy modulation is changed into a spatial modulation or bunching at the input laser's wavelength in the compactor section, and the bunched electron beam radiates coherent light at the fundamental and odd harmonics of the input laser in the radiator section.

The use of a compactor section to enhance bunching has found application in FEL design. This was first proposed by K. Robinson in 1960,[3-2] although the idea was not published until 1977 by Vinokurov and Skrinsky,[3-3] and has since been theoretically examined by several authors.[3-4] Csonka first proposed creating the energy modulation using an external laser in 1978,[3-5] and there has been extensive theoretical work on the production of harmonics using the TOK since then.[3-6] There exist at least two other proposals to implement the TOK on a storage ring to create higher harmonics of a powerful input laser.[3-7] The only reported experimental work on the TOK concept has been from Novosibirsk[3-8] and Orsay,[3-9] although a TOK-style prebuncher was used in a TRW-Stanford FEL experiment.[3-10] The frequency variation of the output intensity as a function of the magnetic field strength in the compactor compares extremely well with theory, and the interference pattern in the emission from two undulators separated by a compactor has been observed. The Orsay group has observed a gain enhancement in the FEL, as expected, and has done preliminary work on the generation of coherent harmonics. (Indeed, the successful operation of the FEL at Orsay in the visible region depended critically upon the gain enhancement produced by the compactor.)[3-11] These experimental studies show that the central principle of the TOK, enhanced bunching of the electron beam at optical wavelengths using a special magnetic compactor section, is in accord with theory.

In the following sections, we explain the general physical principles behind the operation of each of the three sections of the TOK and derive expressions valid in the plane-wave limit for energy modulation, bunch compaction, and radiation of coherent light at the harmonics of the laser. More detailed calculations of conversion efficiencies using Gaussian laser modes have been performed but are beyond the scope of this report and will be reported elsewhere.

3.1 Modulator

The interaction of the electron beam with the laser beam in the periodic field of the undulator produces an energy modulation because the undulator magnet produces a transverse velocity component in an electron's motion that can couple to the laser light. The matching of the laser wavelength, the electron energy, and the undulator period must be correct or no resonant energy transfer between the laser and the electron takes place. In an undulator, a relativistic electron emits synchrotron radiation at a fundamental wavelength

$$\lambda = \frac{\lambda_0}{2\gamma^2}\left(1 + \frac{K^2}{2}\right) , \qquad (3\text{-}1)$$

where λ is the electron energy in rest mass units, λ_0 is the magnet period, and K is the undulator parameter, or dimensionless vector potential, given by

$$K = \frac{\lambda_0 e B_0}{2\pi mc^2} \quad . \tag{3-2}$$

Here B_0 is the peak value of the magnetic field.

If one views the motion of the electron from an inertial frame moving with the average forward velocity of the electron, $v = \beta^* c$, the laser is Doppler shifted to longer wavelengths, and the undulator period is compressed by the Lorentz contraction. The magnetic field of the undulator is boosted by a factor of γ^*, and the moving magnetic field is transformed into a strong electric field, so, in the moving frame, the undulator magnet looks like a very-strong electromagnetic wave, with a period of λ_0/γ^*. The laser wavelength in the moving frame is $\gamma^*(1 + \beta^*)\lambda$. Here,

$$\gamma^* = \frac{1}{\sqrt{1-\beta^{*2}}} \quad . \tag{3-3}$$

The undulator magnetic field reduces the average longitudinal β to

$$\beta^* = 1 - \frac{1 + \frac{K^2}{2}}{2\gamma^2} \quad , \tag{3-4}$$

yielding

$$\gamma^{*2} = \frac{\gamma^2}{1 + \frac{K^2}{2}} \quad . \tag{3-5}$$

In the moving frame, the electron is driven by the sum of the laser field and the transformed undulator field. For small fields, the electron executes simple periodic motion under the influence of the electric field of the undulator wave, since the laser field is very small compared to the boosted undulator field. For large undulator fields, however, corresponding to $K > 1$, the electron is driven to relativistic transverse velocities. The transformed undulator magnetic field then bends the simple harmonic motion into a "figure-eight" curve.[3-12] It is this motion that is responsible for the emission of harmonics of the fundamental frequency given by Eq. (3-1), since, in the moving frame, the electron is actually radiating synchrotron radiation.

When the wavelength of the laser, λ_L, is equal to the spontaneous emission wavelength λ, given by Eq. (3-1), a resonance condition exists. In the moving frame, the laser and undulator wave have the same wavelength at resonance, λ_0/γ^*. Therefore, a weak

modulation of the stationary-standing-wave envelope exists, with a period of $\lambda_0/2\gamma^*$. The amplitude of the standing wave is proportional to the product of the laser electric field and the undulator field. The electron's figure-eight motion causes it to sample different parts of the standing-wave field. This produces a net average force on the electron along the z-direction, proportional to the gradient in the electric field intensity, the ponderomotive force.[3-13] The electron accelerates or decelerates under the influence of this force and can execute bound energy oscillations (synchrotron oscillations) in the ponderomotive potential. If electrons are uniformly distributed along the beam, for a short interaction time in the undulator-laser standing-wave field, electrons gain or lose energy depending on their initial phase relative to the standing-wave pattern. This leads to an expression for the maximum change of energy, measured in the laboratory frame, for a modulator of length $L_0 = N\lambda_0$, given by

$$\Delta E_{max} = \frac{e^2 \lambda_0 B_0 E_L L_0}{4\pi\gamma mc^2} \quad . \tag{3-6}$$

In this discussion, we have neglected the effect that the figure-eight motion has on the Fourier components of the z motion and hence on the ponderomotive force. When this is included, Eq. (3-6) is multiplied by the usual Bessel function factor, which is about unity. The value of ΔE for a given electron depends on its initial phase Φ relative to the laser and undulator fields, thus,

$$\Delta E = \Delta E_{max} \sin \Phi. \tag{3-7}$$

Notice that the energy modulation takes place on a length scale $\lambda_0/2\gamma^*$ in the moving frame, so, transforming back to the laboratory frame, the wavelength of the energy modulation is just

$$\frac{\lambda_0}{2\gamma^{*2}} \quad . \tag{3-8}$$

At resonance this is just λ_L, the laser wavelength. Thus, the interaction of the laser and undulator fields produces a periodic energy modulation with the wavelength of the laser and proportional to the product of the field strengths and the length of the interaction region.

Notice that the maximum energy modulation occurs when the laser is tuned to resonance. Since an equal number of electrons are accelerated and decelerated, there is no net change in the average energy of the electron beam or the laser field. This is also true in a conventional microwave klystron, where, for a monoenergetic electron beam, the energy modulation process is lossless, producing theoretically infinite power gain. In the FEL, net energy gain or

loss is achieved by detuning slightly away from resonance. This causes the standing-wave envelope in the moving frame to drift, and this moving potential pattern can either accelerate or decelerate electrons in the beam, causing a net energy change. In general, the energy modulation effect we have been discussing is much larger than the average energy shift.

It is apparent that for the energy modulation of Eq. (3-6) to have any significance, it must exceed the natural energy spread of the storage ring, σ_ε, given by[3-14]

$$\frac{\sigma_\varepsilon}{E_0} = 4.377 \times 10^{-7} \frac{\gamma}{\sqrt{\rho_0}} . \tag{3-9}$$

Here E_0 is the electron beam energy, and ρ_0 is the bend radius in meters. Using Eq. (3-6), we find that for $\Delta E_{max}/\sigma_\varepsilon$ to be greater than unity a laser power in the megawatt range is required. Such powers are only obtainable from pulsed lasers. Lasers producing pulses with peak power exceeding 100 MW and coherence lengths greater than the electron bunch length are available commercially, however. In practice, a 100-MW, tightly focused laser can produce a modulation $\Delta E_{max}/\sigma_\varepsilon$ greater than 20, so, as we will see later, a significant power output up to about the 20th harmonic should be possible.

3.2 Compactor

The principle of the klystron is that a spatially bunched beam can radiate significantly more power than an unbunched one. It is the function of the compactor section to translate energy modulation into spatial bunching. This is accomplished by the longitudinal dispersion or momentum compaction factor of the bunching section, given by $\alpha = (\gamma/s)\,(\partial s/\partial \gamma)$, where s is the distance traveled by the electron. This produces a path difference ΔS, given by $\Delta S = \alpha L\,(\Delta E/E)$. For free space, $\alpha = (1/\gamma^2)$. This leads to an unreasonably long drift region if free space is used. In an undulator magnet, however, the electrons do not travel in straight paths, and we must use $s = \beta^* ct$ to derive the momentum compaction:

$$\alpha = \frac{\gamma}{s}\frac{\partial S}{\partial \gamma} = \frac{\gamma}{s}\frac{\partial S}{\partial \beta^*}\frac{\partial \beta^*}{\partial \gamma} = \frac{\gamma}{\beta^*}\frac{\partial \beta^*}{\partial \gamma} . \tag{3-10}$$

Using the definitions of β^* and γ^*, Eqs. (3-4) and (3-5), we get

$$\alpha = \frac{1 + \frac{K^2}{2}}{\gamma^2} . \tag{3-11}$$

Thus, the effect of the periodic magnetic field is to increase the effective length by a factor $1 + (K^2/2)$. For $K = 10$ in the

compactor section, something easily accomplished with a large λ_0, the effective length is 51 times larger, so even a single-period undulator can achieve the same bunching as a long region of free space. Hence, a variable-K compactor can be used so that a given physical length will fully bunch a beam with a given energy modulation.

If ΔE is small, then significant compaction will be required, but if ΔE is large, which, as will be seen later, is desirable for good conversion efficiency for the higher harmonics, then the natural α of the modulator and radiator undulators will bunch the beam. To reach the 100-Å range in the TOK using an extremely high-power excimer laser with a short fundamental wavelength, no separate compactor would be required. Such devices are designed to be "integrated" rather than modular, with the energy modulation, bunching, and radiation taking place in a distributed fashion in a single magnet, as shown in Fig. 3-2. In this limit, the system becomes more like an optical traveling wave tube than a klystron.

3.3 Bunching

We are now in a position to calculate the optimal bunching condition and the harmonic content of the bunched beam, following the derivations used by Webster and Slater.[3-3] When the beam exists in the modulator at time t_0, there is very little bunching, and the current is given by $I_0 = e(dn/dt_0)$, where n is number of electrons. The current at the exit of the compactor at time t is

$$I(t) = e\frac{dn}{dt} = I_0 \frac{dt_0}{dt} \quad . \tag{3-12}$$

The time t is related to the time t_0 by the relationship

$$t = t_0 + \frac{L}{\beta^* c} + \frac{\alpha L}{\beta^* c}\frac{\Delta E}{E} \quad . \tag{3-13}$$

Here ΔE is the energy modulation. Using Eq. (3-7) with Φ written as ωt_0, we obtain

$$I(t) = \frac{I_0}{(1 + \eta \cos \omega t_0)} \quad . \tag{3-14}$$

Here $\eta = 2\pi\Delta s/\lambda$, and $\Delta s = \alpha L \Delta E/E$. Note that t_0 is given in terms of t implicitly by Eq. (3-13).

Equation (3-14) describes a current that is bunched at the entrance to the radiator. In fact, Eq. (3-14) describes the adjustment of the compactor to obtain the maximum harmonic content in

the beam: for some t, $\cos \omega t_0 = -1$ and $I(t) \to \infty$ for $n = 1$, i.e.,

$$\alpha = \frac{\lambda}{2\pi L} \frac{E}{\Delta E} \quad . \tag{3-15}$$

Equation (3-15) is the fundamental design equation for the operation of the compactor section.

Fourier expansion of Eq. (3-14) yields the charge density as a function of t and z:

$$\rho(z,t) = \rho_0 \left[1 + \sum_{n=1}^{\infty} a_n \cos \frac{2\pi n}{\lambda} \left(\frac{z}{\beta^*} - ct \right) \right] \quad , \tag{3-16}$$

where

$$a_n = 2J_n(n_n). \tag{3-17}$$

Note that for large n the Bessel function $J_n(x)$ is a maximum when $x \simeq n$, which is just the requirement discussed above to maximize harmonic output, $n = 1$.

3.4 Energy Spread

Up to this point, the initial electron beam has been assumed to be monoenergetic, with no energy spread. Under this assumption, even a vanishingly small energy modulation imposed in the modulator can yield perfect beam bunching if there is sufficient α in the compactor. This is analogous to the fact that the power gain of an ordinary klystron is infinite for a perfectly monoenergetic electron beam. Of course, real electron beams have energy spread, and the higher harmonics in the charge density are reduced by a factor δ_ϵ, where

$$\delta_\epsilon = \frac{1}{\sqrt{2\pi}\,\sigma_\epsilon} \int_{-\infty}^{+\infty} \exp-\left(\frac{\Delta E^2}{2\sigma_\epsilon^2}\right) \cos \left(\frac{2\pi n \alpha L \Delta E}{\lambda E}\right) d(\Delta E)$$

$$= e^{-\frac{n^2}{2n_c^2}} \quad . \tag{3-18}$$

Here n_c is the cutoff harmonic given by

$$n_c = \frac{\Delta E_{max}}{\sigma_\epsilon} \quad . \tag{3-19}$$

The factor δ_ε multiplies the Fourier coefficient a_n in Eq. (3-17). Hence, if the nth harmonic is desired, ΔE_{max} must be greater than $n\sigma_\varepsilon$. This may be viewed either as a requirement on the laser or as a design constraint on the electron storage ring. In addition, if a large energy spread is produced by the laser beam, a significant amount of time must pass for the natural synchroton radiation damping of the storage ring to cool the electron bunch before another laser shot is attempted. If this is not done, the factor δ_ε will reduce the higher harmonic output significantly.

3.5 Angular Spread

Another factor related to the properties of real electron beams spoils the harmonic output. Until now, we have assumed that the electron beam has no angular spread. If an electron moves through the compactor with an average angle θ with respect to the z-direction, in a compactor section of length L it will cover an extra distance $L\theta^2/2$ and thus pick up an extra phase $\pi L\theta^2/\lambda$. If there is a Gaussian distribution of angles in the beam with width σ_θ, then

$$\delta_\theta = \frac{1}{\sqrt{2\pi}\,\sigma_\theta} \int_{-\infty}^{+\infty} \exp\left[-\left(\frac{\theta^2}{2\sigma_\theta^2}\right)\right] \cos\left(\frac{2\pi n}{\lambda}\,\frac{L\theta^2}{2}\right) d\theta$$

$$= [(1 + b)/2b^2]^{1/2}\,, \qquad (3\text{-}20)$$

where

$$b = \left[1 + \left(\frac{2\pi n L \sigma_\theta^2}{\lambda}\right)^2\right]^{1/2}.$$

The factor δ_θ also multiplies the a_n given by Eq. (3-17) and is a measure of how the higher harmonic content of the bunched beam is spoiled by the inherent angular divergence of the stored electron beam. For $\sigma_\theta \simeq 10^{-4}$ radian and for $\lambda = 5320$ Å, L = 1 meter, and n = 11, Eq. (3-20) gives $\delta_\theta = 0.70$. For higher harmonics, $\delta_\theta \sim n^{-1/2}$. This is to be compared with the dependence of δ_ε on n for large n, $\delta_\varepsilon \sim e^{-n}$. Clearly the effect of energy spread in the storage ring on the high harmonics is much more severe than is the effect of angular spread.

The final expression for the Fourier coefficients of the bunched beam at the exit of the compactor is

$$a_n = 2J_n(n\eta)\delta_\varepsilon\delta_\theta. \qquad (3\text{-}21)$$

The design of a specific TOK device reduces essentially to maximizing a_n for the harmonic of interest as the beam enters the radiator.

3.6 Radiator

The normal incoherent radiation from an unbunched beam is enhanced by a large factor when the beam is bunched. Since incoherent radiation is emitted at the fundamental wavelength, given by Eq. (3-1), and its harmonics, the presence of spatial harmonics in the bunching produces an enhancement in the harmonic emission. The enhancement can be shown to be given by

$$\frac{d^2I}{d\omega d\Omega} = |F|^2 \frac{d^2I_0}{d\omega d\Omega} , \tag{3-22}$$

where the left-hand side is the emitted energy per unit solid angle and frequency for the bunched beam, and $|F|^2$ is the coherent enhancement factor, multiplying the emitted energy for a single electron. A simplified view of the derivation of F is that since in the nth spatial harmonic in the beam there are $a_n N_e$ electrons distributed longitudinally in a phase-coherent manner according to $\cos[(2\pi z/\lambda)]$, then the coherent enhancement is just

$$|F|^2 = \frac{1}{2} (a_n N_e)^2 . \tag{3-23}$$

This is because these $a_n N_e$ electrons are all radiating in phase, and, hence, their radiation adds as the square of the number of electrons. Since N_e is very large, on the order of 10^{11} electrons in a single macrobunch, the coherent enhancement can be very large. The source brightness for the radiation emitted is proportional to Eq. (3-22), so one can see that optically bunching the electron beam increases source brightness by the coherent enhancement factor, producing laserlike angular divergence and frequency bandwidth.

To get the total energy emitted, one must multiply Eq. (3-22) by the solid angle and fractional linewidth into which the $a_n N_e$ electrons radiate. For our plane-wave description, where the electron beam is uniformly illuminated by the laser,

$$d\Omega = \frac{\left(\frac{\lambda_L}{n}\right)^2}{(\text{radiating area})}$$

$$= \frac{\lambda_L^2}{n^2 \, 2\pi\sigma_x\sigma_y} , \tag{3-24}$$

where σ_x and σ_y are the one-sigma widths of the electron beam. If we assume that the coherence length of the laser in the modulator exceeds the storage-ring bunch duration, then $d\omega/\omega$ is given by the transform limit of the Gaussian bunch duration:

$$\frac{d\omega}{\omega} = \frac{\lambda_L}{2n\sqrt{\pi}\ \sigma_z} \ . \tag{3-25}$$

Thus we have an expression for the total energy emitted for the nth harmonic:

$$W_n = \frac{d^2 I_0}{d\omega d\Omega}\Bigg|_{\substack{\omega=\omega_n \\ \theta=0}} \frac{N_e^{\,2}\lambda_L^{\,2} c}{8\sqrt{\pi}\ n^2 \sigma_x \sigma_y \sigma_z}\, a_n^{\,2} \ . \tag{3-26}$$

3.7 Comparison with Unbunched Beam in Undulator

We can compare this to the total incoherent radiation of the unbunched beam passing through the same undulator by noting that

$$d\Omega = \frac{\pi}{nN\gamma^{*2}}$$

$$= \frac{2\pi\lambda}{Ln} \ , \tag{3-27}$$

where L is the length of the radiator and N is the number of radiator periods. Also, for the unbunched beam,

$$\frac{d\omega}{\omega} = \frac{1}{nN} \ . \tag{3-28}$$

Suppose, as a worst-case comparison of power levels, that one is able to collect all of the power emitted in either the coherent or incoherent case. Then the ratio of the two is

$$R = \frac{a_n^{\,2} N_e}{n} \frac{\lambda^2}{16\pi^{5/2}} \frac{NL}{\sigma_x \sigma_y \sigma_z} \ . \tag{3-29}$$

To get an estimate of this ratio, assume a fundamental λ of 5320 Å and a radiator of 1 meter, with 20 periods. Also, we use beam dimensions of σ_x = 1.0 mm, σ_y = 0.08 mm, and σ_z = 45 mm. Then,

$$R = 8.4 \times 10^5 \frac{a_n^{\,2}}{n} \ . \tag{3-30}$$

Further, if we were to measure the intensity through an aperture whose solid angle subtended at the undulator were less than that given by Eq. (3-27), the measured ratio would be

$$R = a_n^2 N_e \frac{N\lambda}{4\sqrt{\pi}\,\sigma_z}$$

$$= 5 \times 10^6\, a_n^2 \quad . \qquad (3\text{-}31)$$

Finally, if the light through the small aperture is to be used in an experimental situation in which the absorption linewidth is small compared to Eq. (3-28) (e.g., an atomic resonance), then the power ratio will be just the coherent enhancement factor given by Eq. (3-23). The factor a_n may be estimated by assuming that the laser has imposed sufficient energy modulation so that $n_c > n$. Then, since $J_n(n) \approx n^{-1/3}$ for large n, we have $a_n^2 \approx 4n^{-2/3}$.

3.8 Power Output

The above discussion has presented the essential physics of the TOK in a simplified manner. A real device will use focused laser beams, and the energy gain, momentum compaction, and radiation will be at least partially distributed along the whole device. This calculation has been done, with the details to be reported elsewhere. Figures 3-3 through 3-5 show the efficiencies of harmonic conversion using typical parameters of a real device, in this case, using the design parameters of the NSLS VUV storage ring.

3.9 Difficulties

In the conventional method of pumping a TOK, described above, the input laser wavelength is made equal to λ. There are several difficulties with this, based on engineering constraints:

1. K (through B_0) is related to the magnet gap g and the wavelength of an optimized permanent-magnet undulator by the empirical formula[3-15]:

$$B_0(\text{tesla}) = 3.33 \exp - \left[\frac{g}{\lambda_0}\left(5.47 - 1.8\,\frac{g}{\lambda_0}\right)\right] . \qquad (3\text{-}32)$$

2. The output peak power is proportional to $N^2K^2\lambda_0^2/\gamma^2$, and the energy modulation imposed by the laser is proportional to E_0K/γ, where E_0 is the peak electric field of the laser. To radiate effectively, the energy-modulated beam must bunch optimally somewhere along the length of the undulator; thus, the dispersion, proportional to K^2/γ^2, must be large enough.

3. All of this is subject to the resonance condition [Eq. (3-1)], so λ_0K^2/γ^2 is a constant set by the input laser's wavelength (large K has been assumed, consistent with good harmonic output). Thus, an optimized TOK must have an undulator with small λ_0 and large K.

4. Such an undulator requires a small value of g, by Eq. (3-32). This causes difficulties in the operation of an electron storage ring, especially at the low values of γ required by the present state of the art in high-power lasers, corresponding to electron energies in the 200- to 500-MeV range. For optimal TOK performance in the conventional pumping scheme, the value of g is small enough that an elaborate movable vacuum manifold must be constructed to allow the gap to be opened during storage-ring injection then closed during TOK operation. In addition, the construction tolerances and physical support requirements for an undulator with large K and small λ_0 are severe, significantly increasing construction costs.

A possible solution to these problems lies in pumping the TOK at one of the harmonics in the undulator radiation spectrum. Pumping on the third harmonic, for example, means that the undulator magnet now must merely satisfy Eq. (3-1) for $\lambda = 3\lambda_L$. This allows a value of λ_0 that is three times larger, and Eq. (3-32) then determines a value of g that is much larger for a given K and γ. This value of g is, for all applications of interest, large enough to allow a fixed gap undulator to be installed in most storage rings. Further, the undulator magnet itself is far easier to build because with large λ_0 and increased values of g the manufacturing tolerances are reduced, and the physical support requirements are relaxed.

As with most solutions, the theoretical advantages do not come without some potentially serious practical problems. For example, if one were interested in, say, the 11th harmonic of the input laser at 5320 Å (pumping on the third harmonic), then the output at 484 Å would be a coherent enhancement of spontaneous output at the 33rd harmonic of the undulator radiation spectrum. There is reason to believe that an undulator with sufficiently tight tolerances on the magnetic materials and construction to evidence a 33rd harmonic in its output spectrum may be difficult to build.[3-16] Thus, the harmonic pumping scheme replaces the difficulties of undulator/storage-ring compatibility with a challenge in undulator design and construction.

3.10 References

3-1. D. L. Webster, J. Appl. Phys. 10, 501 (1939); J. C. Slater, Microwave Electronics (Van Nostrand, Princeton, NJ, 1950), p. 222.

3-2. K. W. Robinson "Ultra Short Wave Generation," unpublished (1960).

3-3. N. A. Vinokurov and A. N. Skrinsky, Preprint InP 77-59, Novosibirsk (1977); N. A. Vinokurov, In Proc. 10th Int. Conf. on High Energy Charged Particle Accelerators, Serpukov, 2, (1977) p. 454.

3-4. See, for example, R. Coisson, Part. Acc. 11, 245 (1981).

3-5. P. L. Csonka, Part. Acc. 8, 225 (1978).

3-6. P. L. Csonka, Part. Acc. 11, 45 (1981); V. Stagno, G. Brautti, T. Clauser, and I. Boscolo, Nuovo Cimento 56B, 219 (1980); I. Boscolo and V. Stagno, Nuovo Cimento 58B, 267 (1980); I. Boscolo, M. Leo, R. A. Leo, G. Soliani, and B. Stagno, Opt. Commun. 36, 337 (1981); W. B. Colson, IEEE J. Quantum Electron. QE-17, 1417 (1981); F. DeMartini, Physics of Quantum Electronics (Addison-Wesley, New York, 1980), Vol. 7, Chap. 32; R. Coisson and F. DeMartini, Physics of Quantum Electronics (Addison-Wesley, New York, 1982), Vol. 9, Chap. 42; P. Elleaume, Physics of Quantum Electronics (Addison-Wesley, New York, 1982), Vol. 8, Chap. 5.

3-7. S. Baccaro, F. DeMartini, and A. Ghigo, Opt. Lett. 7, 174 (1982).

3-8. A. A. Artamonov et al., Nucl. Instrum. Methods 177, 174 (1980).

3-9. C. Bazin et al., Physics of Quantum Electronics (Addison-Wesley, New York, 1982) Vol. 8, Chap. 4; J. M. J. Ortega et al., Nucl. Instrum. Methods (to be published); M. Billardon et al., "FEL Experiment," paper presented at the Bendor 1982 FEL Conference; P. Elleaume, "Optical Klystrons," unpublished paper presented at the 1982 Bendor FEL Conference.

3-10. J. A. Edighoffer et al., Phys. Rev. Lett. 52, 344 (1983).

3-11. M. Billardon et al., Phys. Rev. Lett. 51, 1652 (1983).

3-12. E. M. Purcell, unpublished (1972); appears in Proc. Wiggler Workshop, SLAC, H. Winick and T. Knight, Eds., SSRP Report 77/05 (1977).

3-13. F.F. Chen, Introduction to Plasma Physics (Plenum Press, New York, 1974), pp. 256.

3-14. M. Sands, Introduction to the Physics of Storage Rings, Stanford Linear Accelerator Center, Stanford, CA, SLAC-121 (1970).

3-15. K. Halbach, Journal de Physique Colloque C1-211, Tome 44 (1983).

3-16. B. M. Kincaid, "Random Errors in Undulators," accepted for publication in J. Opt. Soc. Am., Sec. B.

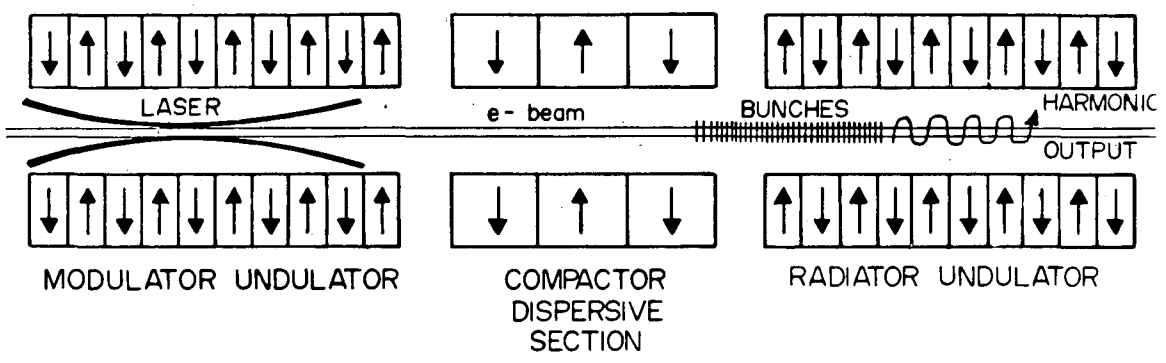

XBL 852-1289

Figure 3-1. Transverse optical klystron.

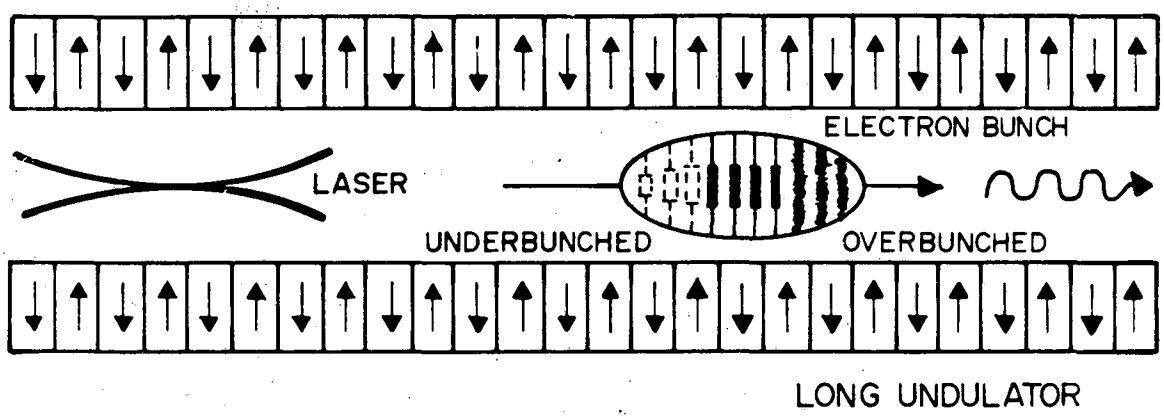

XBL 852-1290

Figure 3-2. Integrated device.

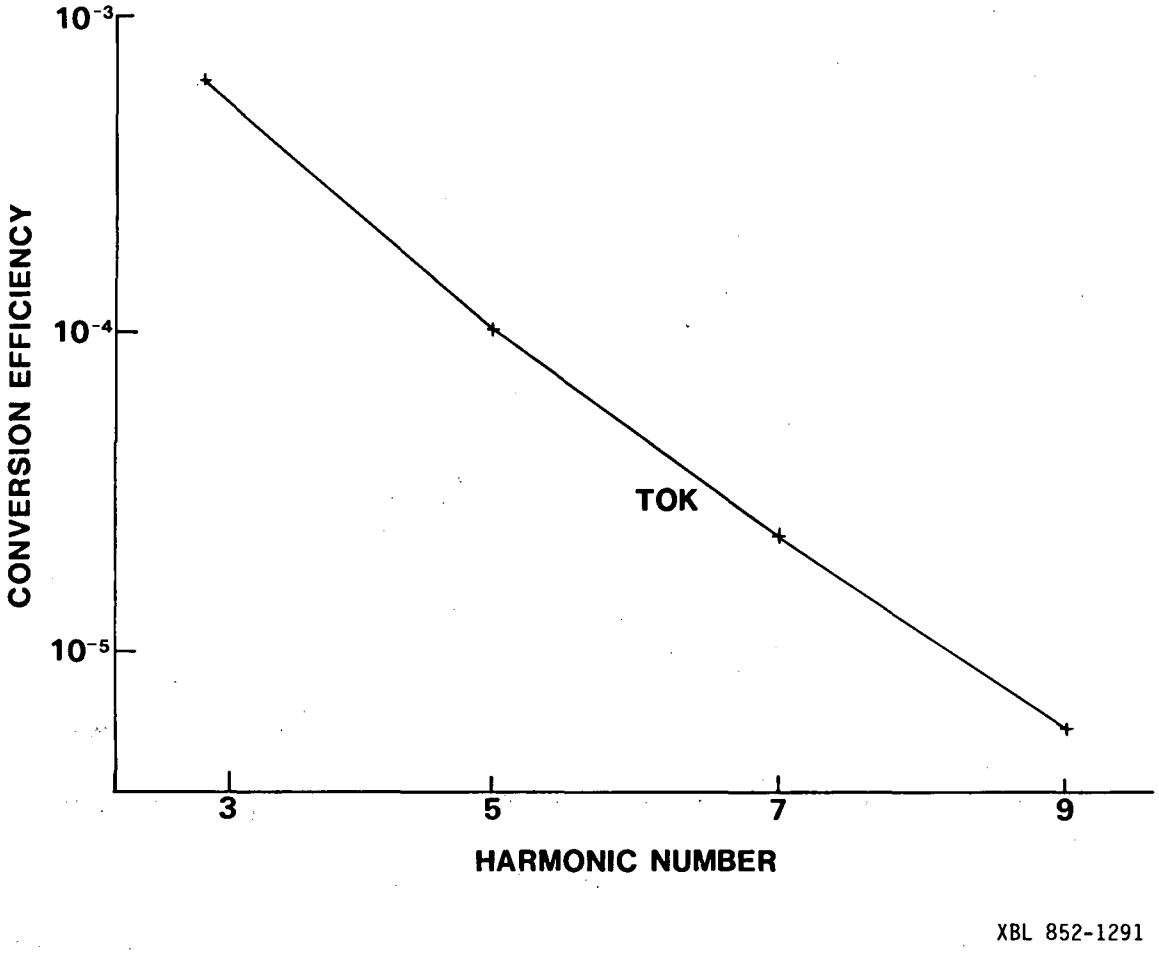

Figure 3-3. Harmonic conversion efficiency for input laser wavelength λ_L = 5600 Å.

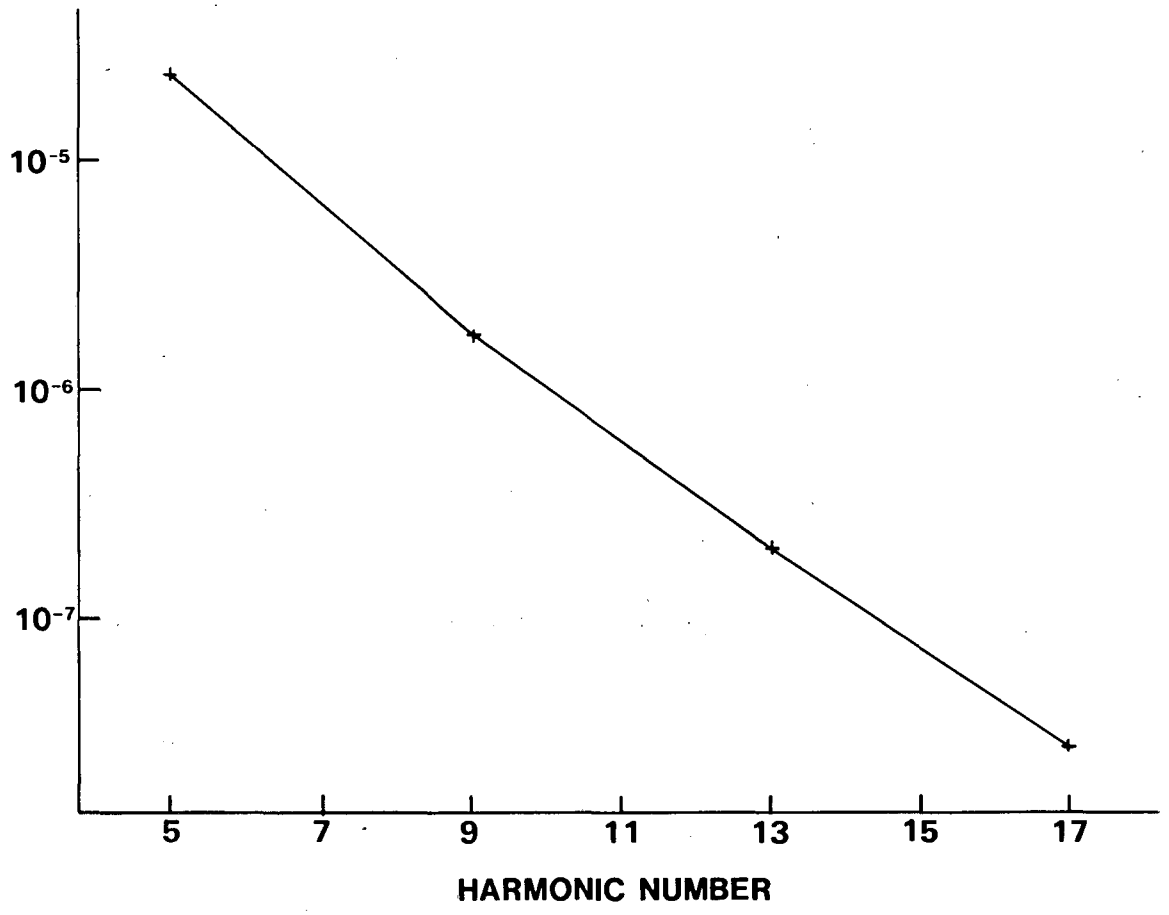

Figure 3-4. Harmonic conversion efficiency for input laser wavelength λ_L = 5320 Å.

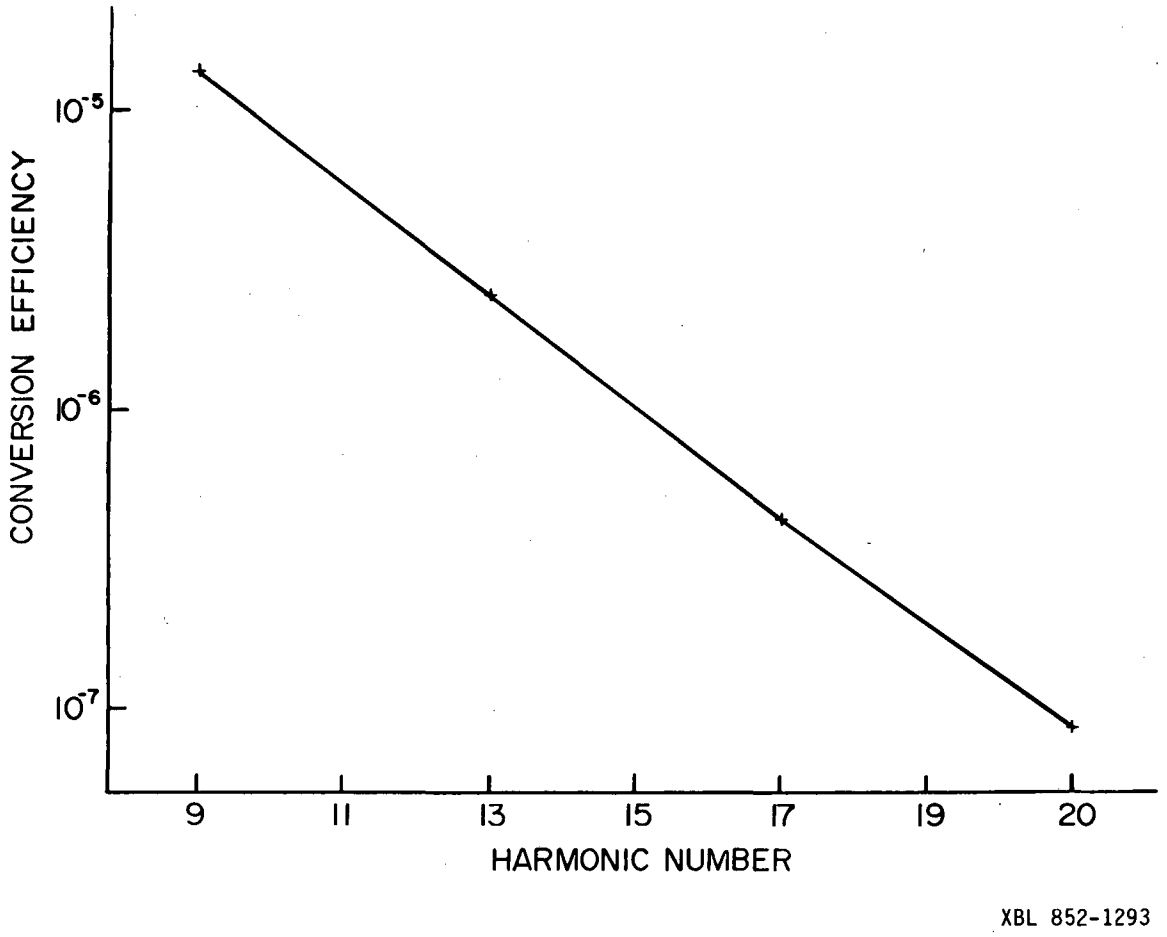

Figure 3-5. Harmonic conversion efficiency for input laser wavelength λ_L = 1.064 μm.

4. FEL Operation at CXF--An Oscillator Configuration

William B. Colson
Berkeley Research Associates

In this section, I consider the problem of generating 500-Å coherent radiation in an FEL oscillator with feedback mirrors. An important advantage in the design of a new storage-ring free electron laser (FEL) oscillator is the research that has already been done at Orsay, France[4-1]; the system there has already been made to work near 5000 Å. An essential item for the success of the oscillator is the availability of suitable mirror surfaces for the resonant cavity. Recent reports of 60% normal-incidence reflectivity in this wavelength range[4-2] give us hope. We will assume 50% reflectivity for the evaluation. The goal in an oscillator configuration is to make the gain/pass greater than the loss/pass, i.e., 4. Once this is accomplished, long-range coherence is established by mode competition. It is expected that the coherence property of radiation from an FEL oscillator would be superior than that of a high-gain FEL amplifier. The main emphasis of this discussion is a valid estimate of gain, based on the following feasible storage-ring parameters:

electron energy = $E = \gamma mc^2$ = 500 MeV
emittance = 6×10^{-7} cm-rad
pulse length = ℓ_e = 2 cm
ring circumference = 180 m
energy spread = $\Delta E/E$ = 0.002
beam radius = r = 0.01 cm
peak current = I = 250 A
two bunches in ring

Below I will present a preliminary FEL design for this hypothetical ring.

To evaluate the importance of short-pulse effects, we need to know the number of periods in the undulator. The electron energy spread $\Delta E/E$ gives a rough estimate for the maximum number of undulator periods, $N \approx E/\Delta E$. For the desired optical wavelength (λ = 500 Å), the dimensionless slippage distance is given by[4-3] $s = N\lambda/\ell_e < E\lambda/\Delta E\ell_e = 10^{-4}$. Such small slippage avoids short-pulse effects, so I will neglect them here.

The storage-ring saturation process creates another interesting pulse problem. At saturation the laser interaction increases the electron energy spread, which, in turn, increases the steady-state electron pulse length. This lowers the electron density and the gain. The final optical pulse is smaller than the electron pulse and is positioned near its middle. The saturated power depends on the synchrotron "cooling" in the ring. The saturated power is P_{sat} =

$P_{syn}/4N$, where N is the number of undulator periods and P_{syn} is the total synchrotron power emitted by the ring. The saturation process is complicated, but it does not have to be solved to estimate whether or not the storage-ring FEL will start.

The classical FEL gain process should be valid at wavelengths like 500 Å. The criterion for quantum effects during the gain process is $\lambda_C N/\lambda\gamma < 1$, where λ_C is the Compton wavelength. For this experiment, $\lambda_C N/\lambda\gamma = 6 \times 10^{-6}$. There is no need to consider quantum effects to estimate the gain process; however, the value of h (Planck's constant) will probably enter into the final determination of the FEL performance, owing to more subtle effects than will be considered here.

The circumference of the ring, 180 meters, contains two electron bunches 90 meters apart. If electrons are to drive the optical pulse on every pass, the mirrors must be 45 meters apart! If the electrons do not drive the light on every pass, the loss/pass is excessively large because of the poor mirrors. With 50% loss/hit, we have only 25% retention per pass. This high loss requires x4 gain/pass to break even; each additional bounce without gain requires another factor of four in gain. If the mirrors were 22.5 meters apart, the minimum gain is x16. The large distance between mirrors requires large mirrors. This may alleviate possible mirror degradation problems, since the flux per unit area would be reduced.

To achieve the desired wavelength, an undulator wavelength of 5 cm is required. The undulator field is made sufficiently strong so that K = 1.0. This is a typical number and can easily be achieved. The effect of an electron energy spread is determined by the number of undulator periods, N. The spread in electron phases at the end of the interaction must be less than π for coherent emission. This requires that $4N\Delta E/E < 1$. For the storage ring assumed here, the largest acceptable number of periods is N = 125. More periods lead to a large gain-degradation effect, which is model dependent; this chosen value of N already leads to significant loss in performance. A brief description of the assumed undulator follows:

undulator wavelength = λ_0 = 5 cm
undulator length = L = 620 cm
undulator K = $eB\lambda_0/2\sqrt{2\pi}\ mc$ = 1.0
number of periods = N = 125.

4.1 Other Parameters

With the number of periods determined, several other variables take on more meaning. The energy spread $\Delta E/E$ gives a spread of π in resonance parameters, as designed, and the emittance gives a spread of 0.9 π. Both of these effects are significant, but more work is needed to assess the performance of an undulator with a larger number of periods and more degredation in gain. The decrease in gain can be

made minimal by reducing the number of periods, but this reduces both the interaction length ($L = N\lambda_0 = 625$ cm) and coupling. This is an important area for further optimization.

Shot noise does not play an important role in the FEL oscillator and can be investigated later. The peak electron density n is 1.7×10^{14} cm^{-3}, which puts 3×10^8 electrons in the important interaction volume element $V = N^2\lambda^2\lambda_0 = 2 \times 10^{-6}$ cm^3. The fluctuations from such a large number are negligible in estimating the gain.

4.2 Performance

The dimensionless current density $j = 8N(\pi eKL)^2 n/\gamma^3 mc^2$, where n is the electron density, is useful in determining the amount of gain and the gain regime.[4-4] For the variables mentioned so far, $j = 180$. When $j >> 1$, the gain is large and collective. However, diffraction and the coupling to the optical mode will have the effect of reducing the gain. Further reduction comes from the energy spread and emittance. If the gain is collective without loss caused by beam quality or mode coupling, then the gain is $G = 1/9 \exp[(j/2)^{1/3}\sqrt{3}] = 265$. If the gain is not collective, then $G = 0.135j$. These are both idealized gain expressions.

To evaluate diffraction and coupling to the optical mode, all transverse coordinates are normalized to the distance $(L\lambda/\pi)^{1/2}$, where $\lambda = 500$ Å is the optical carrier wavelength. This measures the amount of diffraction of the carrier wave over the interaction length L. The transverse diameter of the electron beam in these units is 0.63, which is a little smaller than the normal diffraction width. This is good and is usually hard to achieve at short wavelengths. All longitudinal mode distances are normalized to L. The normalized separation between mirrors is $L_m = 7.2$ or $7.2L = 7.2 \times 6.25$ m = 45 m.

The radius of curvature of the mirrors determines the mode waist at the focus. Because this is a high-gain process, it is best to focus the mode close to the radius of the electron beam. Then self-focusing and high gain will keep the light coupled to the electrons. We chose a normalized Rayleigh length to be $z_0 = 1$, so the normalized mode waist is $w_0 = 1$. The filling factor F is the ratio of the mode volume to the electron-beam volume in the interaction length; for our case, $F = 0.37$. The reduced current density is $jF = 67$. Between the mirrors, the mode is focused so that the mode waist is x3.7 smaller than the mode at the mirrors. Across the resonator length, the mode focuses to 3/4 of the area at the center of the undulator. Then self-focusing and high gain change the shape of the mode at the end of the undulator.

With the resonator designed, we can discuss the capture of spontaneously emitted photons. The transition probability for emitting a photon per electron per pass is 0.7. The probability for

capturing a photon per electron per pass is only 0.2. With the large number of electrons in the important volume element V, we still have a classical field after just one pass. After one pass, the interacting volume contains 7×10^7 photons. Again, the fluctuations are not important. The electromagnetic wave provides a classical force to drive electrons. The fluctuations in the electron current and photon number provide a source of spontaneous emission but would not limit the ultimate coherence of the laser.

Some simulation results can help with the understanding of the problem. Figure 4-1 shows the phase-space evolution of electrons in weak fields. This is optimistic, since energy spread, emittance, and diffraction effects have not been included. Both the gain and optical phase shift are large because $j = 180$ and the gain is collective.

When the filling factor F is used to include diffraction and coupling to the optical mode, the effective j is reduced to 67, as shown in Fig. 4-2.

Diffraction can be calculated as shown in Fig. 4-3. The cross sections of the mode and of the electron beam are followed on the left. High gain and self-focusing are evident in this last figure. The gain and energy in the wavefront are shown on the right. The mode structure at the end of the interaction is plotted in the box at the lower right. This result is with $z_0 = 1$ and $j = 180$.

4.3 Final Thoughts

The conclusion of these brief studies is generally encouraging. When the electron-beam quality (energy spread and emittance) and optical diffraction (mode coupling) are ignored, the system has an excessive amount of gain, and I would suggest that the gain be decreased. It would even be considered an "easy" FEL system to develop. In fact, no experiment to date has demonstrated so much gain. When the energy spread alone is included, the ideal gain is reduced from 265 to 56. When emittance alone is included, the ideal gain is reduced from 265 to 151. When both energy spread and emittance are included, the ideal gain is reduced from 265 to only 40. Diffraction and mode coupling would further reduce the gain. A simple and conservative estimate comes from the filling factor $F = 0.32$, predicting a final gain $G = 15$. Recall that only a gain of 4 is needed to operate the FEL above threshold.

If the above FEL were made and $G = 15$ were actually achieved, it would easily work at 500 Å and below. There are even more tricks that could be used to reach shorter wavelengths or to assure operation at the original design wavelength. Lasing in higher harmonics is an effect seen in most operating FELs, including the storage ring in Orsay. The coupling to higher harmonics depends on the value of K being close to unity, as assumed here. Then there is little decrease in gain at the odd-numbered harmonics. Another trick to raise the

gain in the FEL is to employ a klystron configuration. Here, a dispersive magnetic field is placed halfway along the undulator length to enhance electron bunching in weak optical fields. (See Section 3.) This has also been done in the Orsay experiment. Both the operation in higher harmonics and the klystron configuration are more susceptible to gain degradation caused by electron-beam quality than is the conventional FEL. Although there can certainly be further optimization of the parameters and couplings given here, probably the most important goal of future work on this project should be to maintain and even improve the electron-beam quality quoted.

4.4 References

4-1. M. Billardon et al., Phys. Rev. Lett. 51, 1652 (1983); P. Elleaume et al., J. Physique 45, 989 (1984).

4-2. T.W. Barbee, S. Mrowka, and M.C. Hattrick, "Molybdenum Silicon Multilayer Mirrors for the Extreme Ultra-Violet (EUV)," submitted to Applied Optics, Sept. 1984.

4-3. For notations and definitions of terms used here, and for a review of EFL theory, see W.B. Colson, "Physics of Quantum Electronics," vol. 8, FEL Generators of Coherent Radiation, S.F. Jacobs et al., Eds., (Addison-Wesley, 1982), pp. 457.

4-4. The quantity j here is related to ρ introduced in Section 6 via $\rho N = (j/2)^{1/3}/4\pi$.

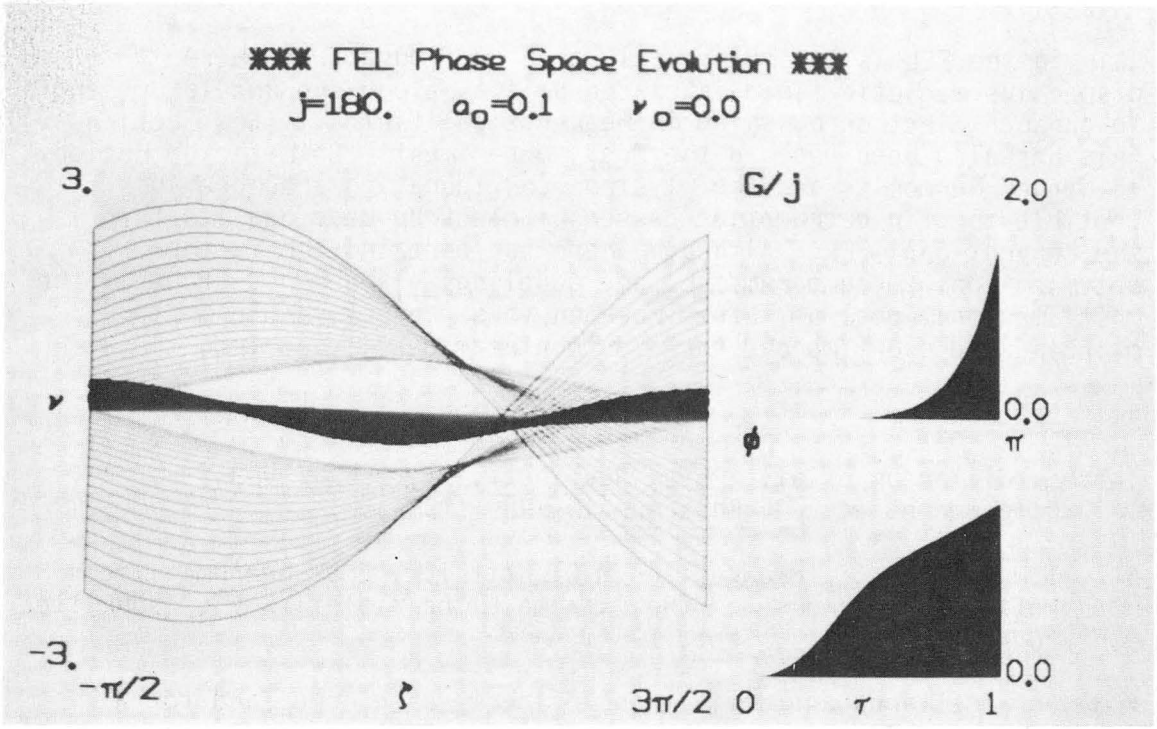

CBB 852-1509

Figure 4-1. Phase-space evolution of electrons in weak field.

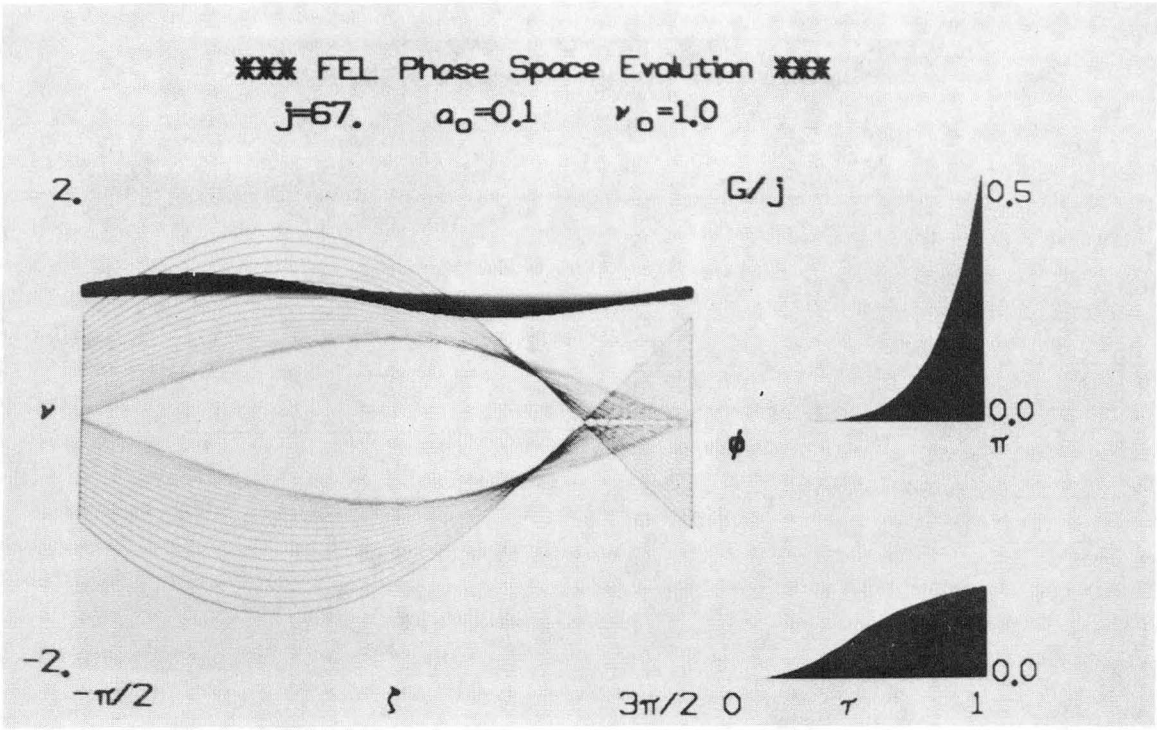

CBB 852-1511

Figure 4-2. Phase-space evolution including diffraction effect.

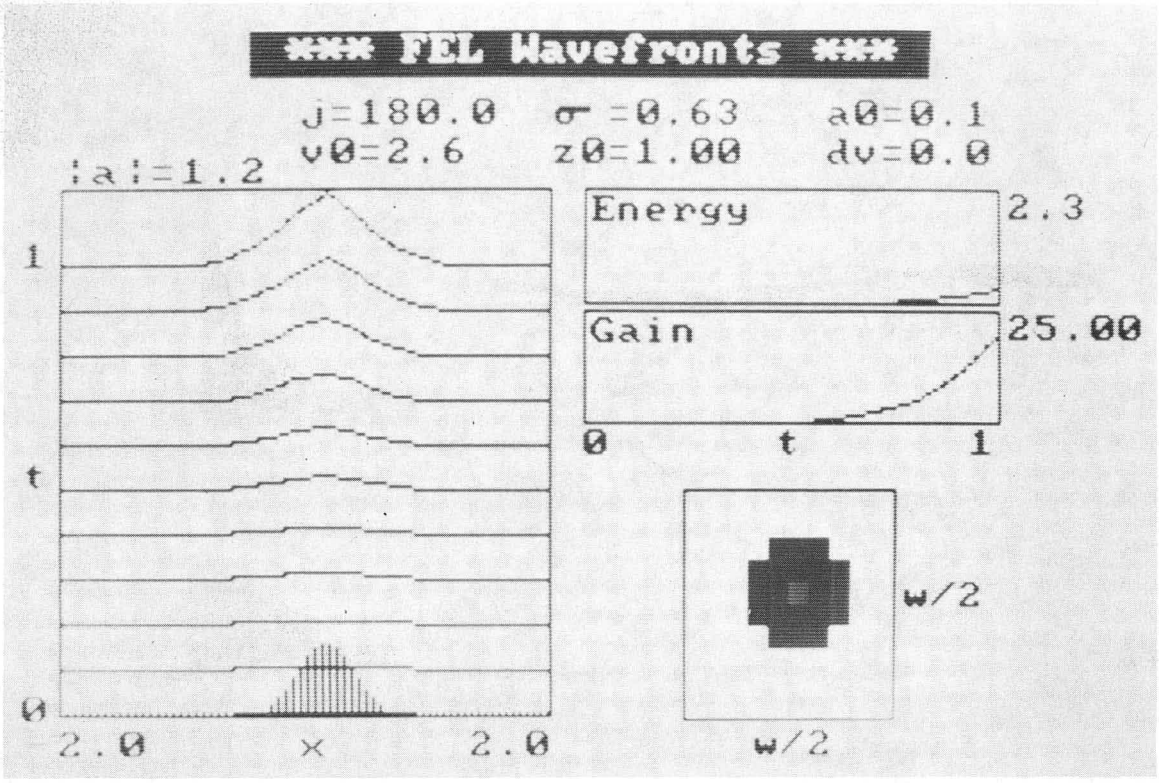

CBB 852-1513

Figure 4-3. Evolution of FEL wavefront.

5. Single-Pass FEL Experiments at LLNL

Donald Prosnitz
Lawrence Livermore National Laboratory

Under certain conditions, the FEL interaction generates enough gain to produce significant amounts of radiation with only a single pass of the electron beam through the wiggler. This occurs if the electron beam has a very high phase-space density (brightness). Furthermore, if the wiggler can be made sufficiently long, the amplifier can be made to saturate on its own noise. The length of the wiggler is limited by diffraction of the optical beam, which eventually reduces the FEL gain. However, refractive phenomena have been predicted that will greatly reduce the detrimental effects of diffraction. A high-current electron beam is required to demonstrate refractive guiding in an FEL.[5-1]

To date there are no electron beams bright enough to drive a far-ultraviolet FEL. However, the required electron-beam brightness is greatly reduced at longer wavelengths. We have taken advantage of this scaling to build a microwave FEL that demonstrates high (exponential) single-pass gain.[5-2] This experimental facility [the Electron Laser Facility (ELF) at Lawrence Livermore National Laboratory] allows us to verify our models of FEL operation and confirm that very high gain can be obtained. Unfortunately, refractive guiding cannot be demonstrated at this facility because at millimeter wavelengths diffraction dominates all other effects.

The ELF wiggler is 3 meters long (30 periods). We have put a 450-A, 3.3-MeV beam through this wiggler and measured the small signal gain at 34.6 GHz. The cold-beam model predicts a gain of 40 dB/m under these circumstances. However, given the finite emittance of our beam and the slight mismatch of the beam into the wiggler, we expect about 15 dB/m. The results of our experiments are shown in Fig. 5-1. The gain is exponential over three orders of magnitude, and the 13.4-dB/m gain is in very good agreement with theory. We obtain about 2 kW of output power when we let the signal grow from noise. The 3-meter amplifier is unsaturated when started from noise. We can therefore obtain more output power if we inject a microwave signal. The saturated output power has been demonstrated to be 100 MW, or about 85 dB above the estimated input noise level of 0.35 W. Our numerical model FRED[5-3] has been very successful (30% error) at predicting the saturated power levels. If the wiggler were 6 meters long, it would saturate on its own noise. Equivalently, if the beam were better matched to the wiggler or brighter, it would saturate with a shorter wiggler. Both of these approaches (a 4-m wiggler and a brighter electron beam) will be pursued during the next year.

We have thus far demonstrated that high single-pass gain can be achieved with an FEL. What is even more important is that we can predict the observed gain as a function of beam quality.

References

5-1. E.T. Scharlemann, A.M. Sessler, and J.S. Wurtele, "Optical Guiding by a Free Electron Laser," Proceedings of Workshop on Coherent and Collective Propagation of Relativistic Electron Beams and Electromagnetic Radiation, Villa Olmo, Como, Italy (Sept. 1984);
G.T. Moore, "The High-Gain Regime of FEL," the same proceedings.

5-2. T.J. Orzechowsky, et al., "Microwave Radiation from High-Gain FEL Amplifier, submitted to Phys. Rev. Lett.

5-3. W.M. Fawley, D. Prosnitz, and E.T. Scharlemann, Phys. Rev. A30, 2472 (1984).

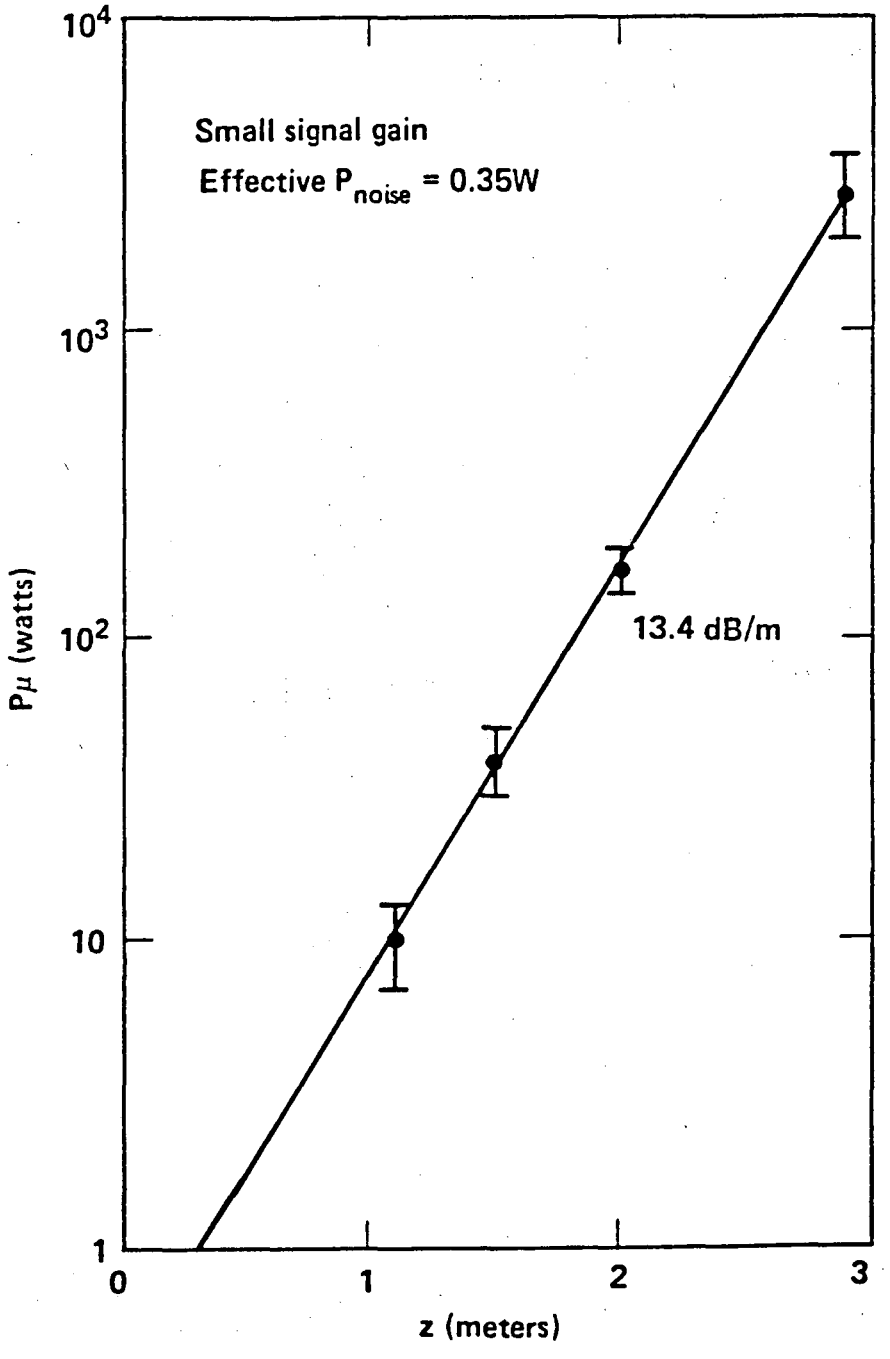

XBL 852-1294

Figure 5-1. Evolution of microwave intensity in ELF experiment.

6. Self-Amplified Spontaneous Emission

Claudio Pellegrini
Brookhaven National Laboratory

The self-amplified spontaneous-emission mode of operation of a free electron laser (FEL) is based on a remarkable property of the undulator/electron-beam radiation system: when the radiation field is small or zero, there is a range of parameters for which the system is collectively unstable. This collective instability leads to an exponential growth of the radiation field and of the beam bunching at the radiation wavelength, until the system saturates.[6-1] This offers the possibility of operating an FEL in a configuration in which the electron beam is simply sent through the undulator; the noise current present in the electron beam is enough to start the exponential growth and, given the right beam and undulator parameters, to produce at the undulator exit a large amount of coherent radiation. We call this mode of operating an FEL "self-amplified spontaneous emission" (SASE).

6.1 SASE: Advantages and Disadvantages

The SASE mode offers the possibility of producing large radiation power pulses starting from noise in the electron-beam current; in fact, the peak power obtainable is larger than in the case of an oscillator or transverse optical klystron (TOK). SASE further eliminates the need for the optical cavity in the oscillator mode of operation or for the external laser beam of the TOK. This is particularly important for the production of XUV radiation (at wavelengths smaller than 1000 Å), since in this region the construction of an efficient optical cavity presents serious problems.

Compared with the TOK, SASE offers the advantage of much larger peak power, eliminates the need for using a powerful laser to modulate the beam energy, and, since it operates on the first harmonic, requires less-stringent undulator tolerances.

The principal disadvantage of SASE is that, to be effective, it requires a large electron-beam density and a long undulator. If we characterize the FEL system by the gain that one can get in an amplification mode, one can see that SASE requires a larger gain than that needed for an oscillator, also when using a low-efficiency cavity, e.g., Q about 4. Following the work of Ref. 6-1, one can characterize the undulator/electron-beam system with a single parameter ρ, defined as

$$\rho = \left(\frac{K\lambda_u\Omega_p}{8\pi c}\right)^{2/3} ,$$

where K is the undulator parameter, λ_u its period, c the velocity of light, and Ω_p the relativistic electron plasma frequency. This last parameter is defined using the electron-beam density n_o and the electron energy γ, measured in rest-energy units, as

$$\Omega_p^2 = 4\pi r_e c^2 n_o/\gamma^3 ,$$

where r_e is the classical electron radius. For a system starting from noise, the radiation-field amplitude and the beam bunching at the radiation wavelength will grow as $\exp(4\pi\rho N_u)$, where N_u is the number of periods in the undulator, provided that the beam energy spread is smaller than ρ.[6-1] Because of saturation effects, the radiation intensity peaks when $\rho N_u \approx 1$. For a longer undulator, the radiation intensity would oscillate around a value smaller than the peak value, unless one modifies the undulator, introducing for instance a tapering of the period. At the radiation peak, the amount of beam energy (U_B) transferred to the radiation is simply given by ρU_B.[6-1] The growth of the field amplitude versus $\tau = 4\pi\rho N_u$ is shown in Fig. 6-1.

To increase ρ, it is important to use an electron beam with a small emittance. In addition, the emittance contributes an additional effective energy spread that has to be smaller than ρ in order not to reduce the growth rate. This last condition can be written as

$$\left(\frac{\Delta E}{E}\right)_{eff} = \frac{1}{2}\left(\frac{2\pi}{\lambda_u}\right)^2 \frac{K^2}{1+K^2}\,\varepsilon_V\beta_V + \frac{\gamma^2}{1+K^2}\left(\frac{\varepsilon_H}{\beta_H} + \frac{\varepsilon_V}{\beta_V}\right) < \rho \quad , \qquad (6\text{-}1)$$

where ε_H, ε_V, β_H, and β_V are the horizontal and vertical emittances and beta functions in the undulator.

6.2 Emittance and Diffraction Effects

When the emittances are small, the beam transverse dimensions are small and diffraction effects can become important, reducing the exponential growth rate to a value smaller than $4\pi\rho N_u$. For radiation at wavelength λ and for a cylindrical beam of radius a, one could estimate the order of magnitude of this effect by comparing the beam radius to the diffraction angle, $\theta = \lambda/a$, multiplied by the undulator length, $L_u = N_u\lambda_u$. Introducing the Raleigh range $Z = \pi a^2/\lambda$, the condition for diffraction to be negligible could then be written as $Z/L_u \geq 1$. It is very important to notice that this condition can be relaxed because of another important property of the FEL systems: the radiation produced by the beam is focused by the beam into itself, thus reducing diffraction effects.[6-2,6-3] This self-focusing effect can be described by saying that the FEL has an effective Raleigh range $Z_{eff} = Z(4\pi\rho N_u)$, so that increasing the beam density increases the beam-focusing effect, as well as the instability growth rate. Using this effective Raleigh range, one can

say that the exponential growth rate is given by $4\pi\rho N_u$ if the condition $Z_{eff}/L_u \geq 1$ is satisfied. How the growth rate is reduced when this condition is not satisfied is described in Refs. 6-2 and 6-3.

6.3 An Example

For a low-energy electron beam and long-wavelength radiation, the parameter ρ can be on the order of 10^{-1}, whereas for a beam in a storage ring and in the XUV region, it can be on the order of 10^{-3}. If we want to reach the peak of the radiation intensity we must have an undulator with several hundred periods. Let us assume that we have $\rho = 2 \times 10^{-3}$ and $N_u = 500$ and that the undulator parameter is $K = 1$. To keep the undulator length small and to have a short wavelength, we want a small undulator period, say $\lambda_u = 1$ cm, and a correspondingly small gap, $g = 2$ mm. The short undulator allows us to focus the beam onto a smaller transverse area, thus increasing ρ. It would also produce 100-Å radiation with a 511-MeV electron energy. For a beam peak current of 100 A the beam peak power is 50 GW, and for $\rho = 2 \times 10^{-3}$, this would give a radiation peak power of 100 MW, provided the effective beam energy spread is less than ρ. Unfortunately, an undulator with such a small gap cannot be inserted into a storage ring without reducing the beam lifetime to almost zero. The solution to this dilemma is to use a ring bypass.[6-4] The use of a bypass for an undulator offers a number of advantages, since it decouples the ring and the undulator and allows independent optimization of the two systems. In such a system, which is shown schematically in Fig. 6-2, one can envisage routing the beam through the bypass once every few radiation damping times to produce an intense radiation pulse, with peak power in the range of megawatts. The average power would still be on the order of ρ times the average synchrotron radiation loss of the beam, as for an oscillator.

In conclusion, the SASE mode, in combination with a bypass on a storage ring, offers a powerful method to produce large peak power, on the order of tens of megawatts in a wavelength region extending down to 100 Å, and allows an FEL system to operate in regions where mirrors are not available, thus greatly expanding the possibility of producing coherent radiation from a relativistic electron beam.

6.4 References

6-1. R. Bonifacio, L. Narducci, and C. Pellegrini, Opt. Commun. 50, 373 (1984).

6-2. E. T. Scharlemann, A. M. Sessler, and J. S. Wurtele, "Optical Guiding by a Free Electron Laser," Proceedings of Workshop on Coherent and Collective Propagation of Relativistic Electron Beams and Electromagnetic Radiation, Villa Olmo, Como, Italy (Sept. 1984).

6-3. G.T. Moore, "The High-Gain Regime of FEL," Proceedings of Workshop on Coherent and Collective Propagation of Relativistic Electron Beams and Electromagnetic Radiation, Villa Olmo, Como, Italy (Sept. 1984).

6-4. J.B. Murphy and C. Pellegrini, J. Opt. Soc. Am. 1B, 530 (1985).

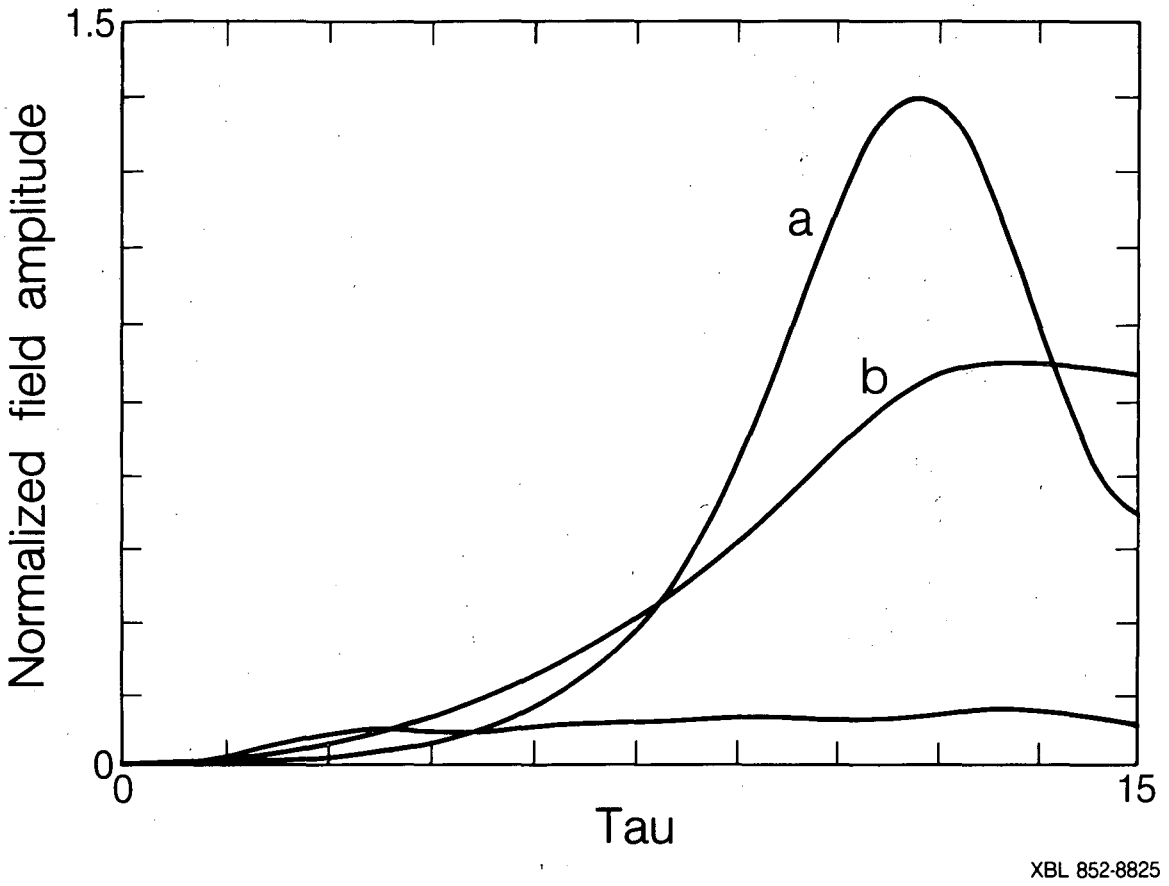

Figure 6-1. Growth of normalized field amplitude as function of τ.

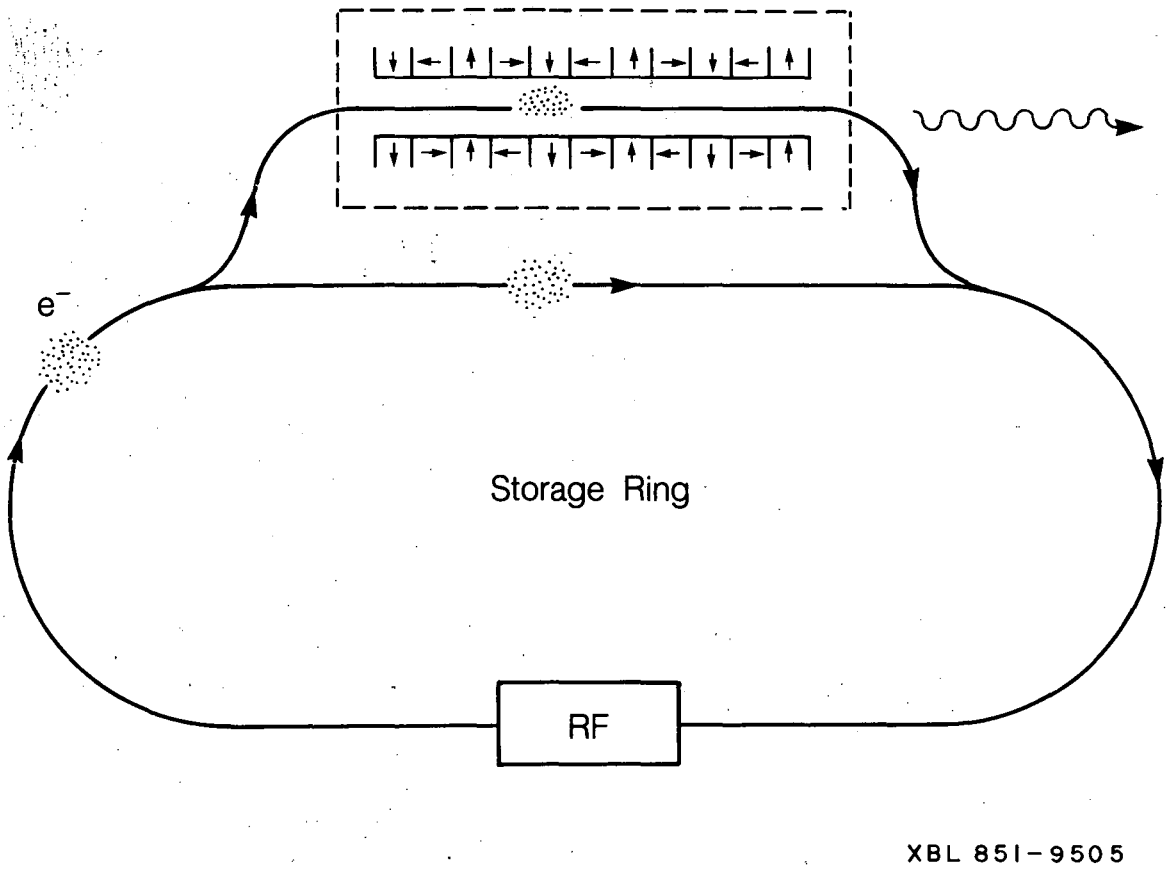

Figure 6-2. Operation of a high-gain FEL in a bypass of storage ring.

7. LATTICE

Alper A. Garren
Lawrence Berkeley Laboratory

The lattice for Coherent XUV facility is designed to operate in two modes. As a source of radiation from undulators it will be run at 1.3 GeV. Low emittance and long straight sections for the undulators are needed. For free electron laser (FEL) experiments the ring will run at lower energy, 0.5 to 0.75 GeV, and the beam must be of high intensity and have small emittance and energy spread.

To have optimum performance for these two modes, tuning flexibility must be assured. In addition, the lattice design must provide adequate spaces for insertion devices, rf, injection and extraction kickers (for the bypass), sextupoles, and orbit-correction equipment.

7.1. Lattice Description

Figure 7-1 shows the ring and bypass. Each of the three superperiods has one long straight section for undulators, bypass, etc., and another for damping wigglers and two achromats.

A schematic of half of one of the symmetric superperiods is shown in Fig. 7-2. It runs between the centers of a 15-m straight section and a damping-wiggler straight section and contains one achromat. The quadrupoles Q4 Q5 Q5 Q4 produce zero dispersion at the ends of the outer dipoles and a horizontal beam waist in the dipoles that give low emittance. The triplet Q1 Q2 Q3 and the doublet Q6 Q7 produce waists in the center of the long straight section and of Q7, which are symmetry points of the ring lattice.

7.2. Explanation of Lattice Design

An electron ring that contains N achromats and no wigglers, and in which β_x is focused in an optimum manner in the dipoles, will have a natural emittance[7-2]

$$\epsilon_{min} = 2.94E(\text{GeV})^2 N^{-3} \text{ mm-mrad.}$$

Thus, low emittance can be obtained by having a sufficiently large number of archromats; for N = 6, ϵ_{min} = 0.008 mm-mrad.

For FEL operation, high intensity and small energy spread are needed, a combination that calls for high momentum compaction α to assure longitudinal stability. The momentum compaction of the N achromat ring is given by

$$\alpha = \frac{\pi^2}{12} \frac{\rho}{R} \frac{1}{N^3},$$

where ρ and R are the magnetic and average radii. Since N is large to reduce the emittance, and R is hard to reduce, given the need for long straight sections, etc., one is forced to make ρ large, that is, to have low-field dipoles. Unfortunately, these do not give short enough damping times to prevent emittance growth from intrabeam scattering. The energy damping time is given by

$$\tau_E(\text{msec}) = 0.24 \frac{R(m)\rho(m)}{E^3(\text{GeV})} ,$$

and reduction of ρ is not possible without also reducing the momentum compaction.

7.3. Damping Wigglers

A way out of the above dilemma is to introduce damping wigglers, as shown in Fig. 7-1, in three straight sections. Because of the achromats, the dispersion is zero at the ends of the wigglers. If β_x is suitably focused in the wigglers by the adjacent quadrupoles, and if the wiggler period length is not too long, the emittance will be reduced by the wigglers. The momentum compaction is not changed appreciably by short-period wigglers. The wigglers shorten the damping time in the ratio

$$\frac{\tau_E}{\tau_{EW}} = 1 + \frac{\Theta_W B_W}{2\pi B_0} ,$$

where Θ_W is the total bend angle in all of the wigglers, B_W their field strength, and B_0 the field of the dipoles. To get the most from these wigglers they should be run at peak field at both operating energies. As a result their vertical focusing effect is greater at low energy than at high, so that the strength of the neighboring quadrupoles must also be different.

7.4. Correctors and RF Cavities

Each achromat contains three chromaticity correcting-sextupoles. Their strength is moderate because the dispersion is rather high in them--a good consequence of the low-field dipoles. The lattice contains drift spaces at appropriate phases for orbit-correcting kickers and monitors. The rf cavities will be placed in some of the 2.5-m spaces adjacent to the triplets.

7.5 Long Straight Sections

The three 15-m straight sections are used for injection, transfer to and from the bypass, and undulators. As a result there will be three spaces available for undulators with approximate lengths of 5, 10, and 15 meters. In addition, there will be radiation from the damping wigglers at three locations.

7.6 Bypass

Figure 7-1 shows the relationship between the ring and the bypass. The transfer is initiated by firing kickers at the ends of two long straight sections that kick the beam into septum magnets. The remainder of the bypass is devoted to bending and quadrupole magnets and the FEL undulator (about 20 meters). If necessary, jitter in the kickers could be partly cancelled by introducing additional kickers 180 degrees away in the bypass.

7.7 References

7-1. R. Chasman and G. K. Green, BNL 50595 (J. P. Blewett, Ed. Vol. 1 (1977), pp. 4-4 to 4-8.

7-2. This and other formulae in this paper are derivable from those given in M. Sands, "Introduction to the Physics of storage Rings," SLAC-121 (1970).

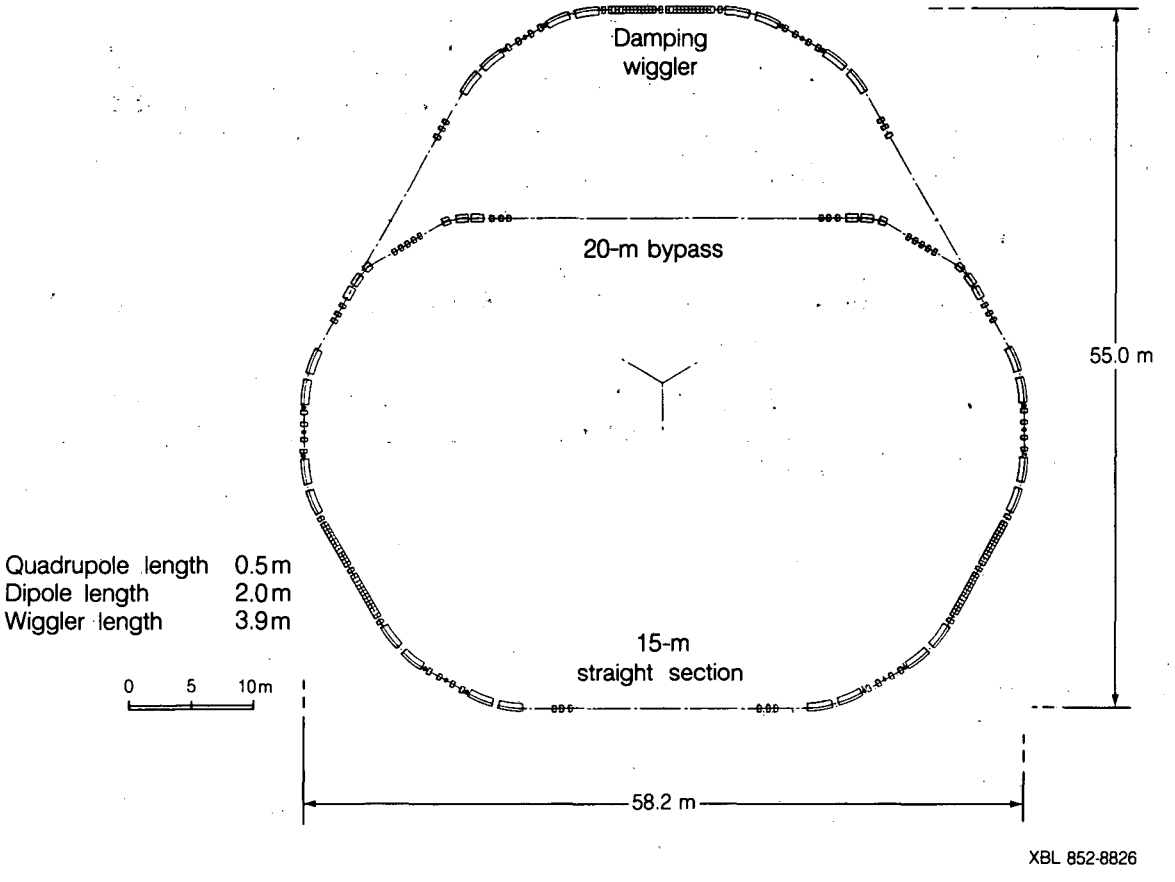

Figure 7-1. Storage-ring/bypass design.

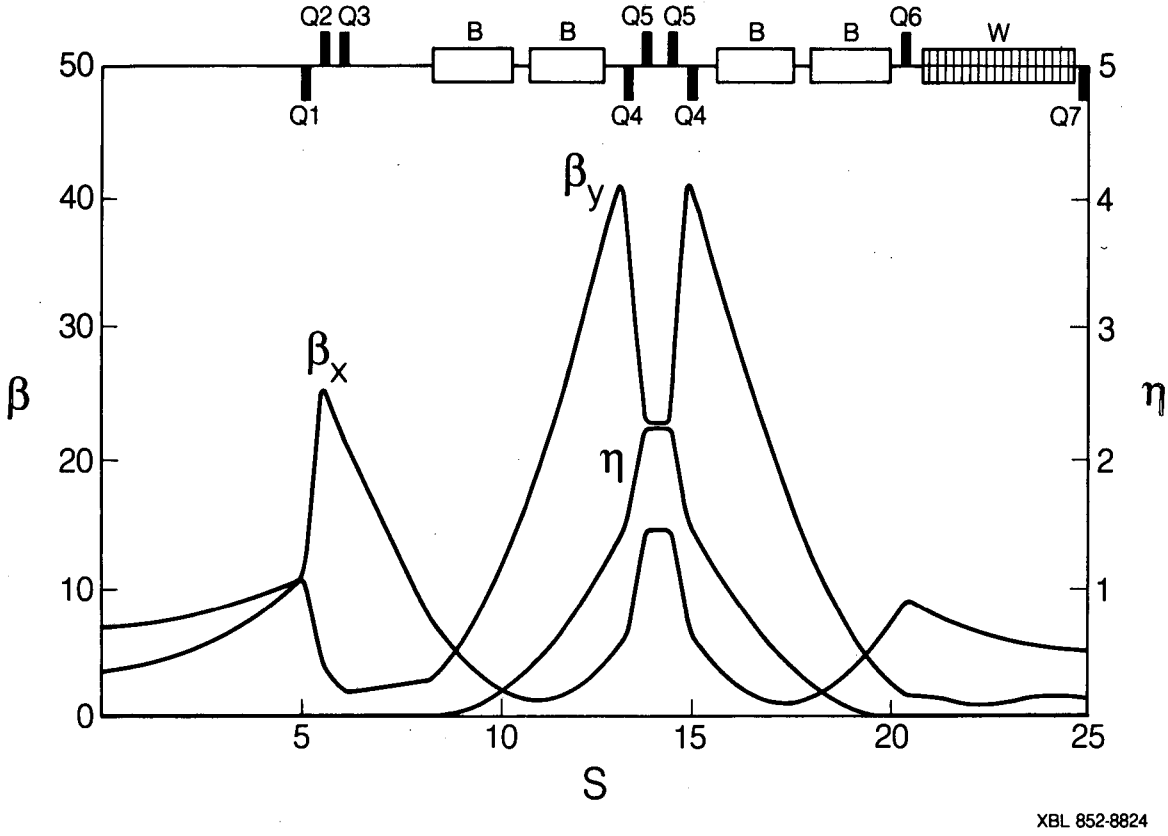

Figure 7-2. The betatron and dispersion functions.

8. COLLECTIVE EFFECTS FOR AN FEL STORAGE RING

Joseph J. Bisognano
Lawrence Berkeley Laboratory

High-performance operation of a free electron laser (FEL) requires a stored beam with both significant volume density (large peak current and small emittance) and low momentum spread. These conditions place severe demands on storage-ring design, which must address the impact of both coherent and incoherent multiparticle phenomena.

The one-dimensional theory of high-gain FEL operation predicts exponential growth of signal and a saturation power level. The e-folding length for growth of radiation power is[8-1]

$$\ell_e = \frac{\lambda_w}{8\pi\rho\, f(\sigma_p/\rho)} \quad , \tag{8-1}$$

where λ_w is the wiggler period and ρ is the FEL gain parameter, which, for a planar undulator, is given by

$$\rho = \left\{ \frac{K^2\,[J_0(\mu) - J_1(\mu)]^2 \lambda_w^2 n_e r_e}{16\pi\gamma^3} \right\}^{1/3} \tag{8-2}$$

Here, K is the usual undulator parameter; r_e, the classical electron radius; n_e, the electron volume density; and $\mu = K^2/(1 + K^2)$. The function f is a form factor that decreases with increasing fractional rms momentum spread σ_p. The saturation power level is found to be on the order of $I_p(E/e)$, where I_p is the peak current and E is the electron energy.

From the storage-ring designer's point of view, the FEL demands maximization of the bunched-beam volume density, or, equivalently,

$$n_e = \frac{N}{\sigma_x \sigma_y \sigma_\ell} \propto \frac{I_p}{\sqrt{\epsilon_x \epsilon_y}} \propto \frac{I_p}{\epsilon_x} \tag{8-3}$$

where N is the number of particles per bunch; ϵ_x and ϵ_y are the horizontal and vertical emittances, respectively, and σ_x, σ_y, and σ_ℓ are the rms beam dimensions. In addition, there is the added constraint of

$$\sigma_p < \rho \ , \tag{8-4}$$

since $f(\sigma_p/\rho)$ degrades considerably for $\sigma_p/\rho > 1$. This requirement for high 6-D phase-space density enhances the impact of multiparticle effects, including both coherent instabilities and intrabeam scattering. The following discussion characterizes these phenomena in some detail.

8.1 Coherent Instabilities and Machine Impedance

The interaction of the beam current with its environment can produce electromagnetic fields that, in turn, affect the beam. This feedback can generate a variety of coherent instabilities that limit beam current. These electromagnetic fields can be generated by beam excitation of rf cavities, vacuum chamber discontinuities, and wall resistivity; in addition, the process of synchrotron radiation produces self-fields. These interactions are summarized in terms of frequency-dependent longitudinal and transverse impedances.

The threshold peak currents for longitudinal and transverse single-bunch instability are given, respectively, by the expressions[8-2]

$$I_p^L = \frac{2\pi\,\alpha\,\sigma_p^2(E/e)}{(Z/n)_{eff}}\,F_L \tag{8-5}$$

and

$$I_p^T = \frac{4\sqrt{2}\pi(E/e)\nu_s}{eZ_T\beta}\,F_T\,, \tag{8-6}$$

where α is the "frequency-slip" factor; ν_s, the synchrotron tune; and F_L and F_T are form factors on the order of unity. The effective longitudinal (Z_n/n) and transverse (Z_T) impedances are averages of the full frequency-dependent impedances over bunch-mode spectra. For typical FEL storage-ring parameters, the longitudinal threshold is usually the more severe limit.

Observations at SPEAR are consistent with[8-3]

$$\frac{Z}{n} = \left(\frac{Z}{n}\right)_0\left(\frac{\sigma}{b}\right)^{1.68} \tag{8-7}$$

for σ less than the effective pipe radius b and $(Z/n)_0 = 10\Omega$. For $\sigma > b$, $(Z/n) = (Z/n)_0$.

With smooth vacuum-chamber construction, small rings such as the NSLS VUV machine have achieved $(Z/n)_0 \simeq 1$ or 2Ω. Short bunch lengths [for high peak current and minimization of (Z/n) through Eq. (8-7)] require substantial rf systems, which can increase $(Z/n)_0$ by an ohm or more. Thus, the benefits of shorter bunch lengths (in lowering the effective impedance) can be diminished. Moreover, for small storage rings (~100 meters in circumference), there is another important source of self-interaction, namely, the radiation process. A long electron bunch does not radiate coherently because of shielding provided by the vacuum pipe. For wavelengths considerably shorter

than the beam-pipe dimensions, this shielding effect no longer occurs. A short coherent modulation of the bunch current will produce synchrotron radiation, and electrons experience a radiation-reaction longitudinal electromagnetic field. This effect has been found to be well approximated in several geometries by an impedance[8-4]:

$$(Z/n) = 300 \frac{h}{R} \ (\Omega) \ , \tag{8-8}$$

where h is the beam-pipe half-length and R is the storage-ring radius. For a 15-m-radius ring, with a pipe half-height of 2.5 cm,

$$(Z/n) = 0.5 \ (\Omega) \ . \tag{8-9}$$

For smooth, small rings, this "free-space" impedance often sets a lower limit on the longitudinal impedance. For a closed vacuum pipe the impedance caused by the synchrotron radiation will have a resonant character, and Eq. (8-8) provides a rough, smeared-out average. Further efforts, both analytical and experimental, are required. It should be noted that although instability driven by the synchrotron radiation impedance has probably been observed in electron-ring experiments, the nature of this instability relative to bunch lengthening, momentum stabilization, etc., in storage rings has not been studied. Figure 8-1 summarizes the various contributions to broadband impedance discussed so far. Finally, from Eqs. (8-5) and (8-9) we find that a 500-MeV, 100-m-circumference storage ring with $\alpha = 0.01$ will have a peak current limit

$$I_p^L = 251 \ A \tag{8-10}$$

for $\sigma_p = 0.002$.

8.2 Intrabeam Scattering

Coulomb scattering of electrons within the beam can lead to excitation of betatron and energy oscillations. For large-angle scatters, an electron's momentum error may exceed the acceptance of the lattice or rf bucket. The particle is lost, with a resulting lifetime limitation of the beam (Touschek effect). Multiple intrabeam scattering, however, causes both longitudinal and transverse diffusion, which, for insufficient synchrotron damping, can lead to emittances well above the quantum excitation level. The theory of multiple intrabeam scattering has been developed most fully in the work of Piwinski[8-5] and of Bjorken and Mtingwa.[8-6] The detailed formulations require numerical evaluation of rather involved expressions for diffusion rates. In the following, attention will focus on the basic physical principles and on simple (limited) scaling laws derived from numerical evaluation of some typical FEL storage-ring parameters.

In the beam frame, the horizontal momentum spread is typically larger than the longitudinal; Coulomb scattering dominantly transfers momentum from horizontal into longitudinal. However, in dispersive regions of the ring, the closed orbit moves with changing momentum, and horizontal betatron oscillations can be excited. For large enough dispersions, the betatron excitation more than compensates for the loss of transverse momentum in the basic scattering event. In fact, it appears that, for many small, low-energy lattices for synchrotron radiation sources, the horizontal diffusion rate is the larger. The so-called H-function

$$\mathscr{H} = \gamma\eta^2 + 2\alpha\eta\eta' + \beta(\eta')^2 \ , \tag{8-11}$$

where α, β, γ, and η are the usual synchrotron lattice functions, is the primary factor in determining transverse diffusion.

If, for a given emittance, the intrabeam scattering diffusion rate exceeds the synchrotron damping rate, emittance growth will occur until the diffusion from scattering and quantum fluctuation matches the damping rate. For a class of lattices that has been recently considered for FEL use, the horizontal diffusion rate was found to be given approximately by

$$\frac{1}{\tau_x} = C\,\frac{I_p}{\varepsilon_x^2}\left(\frac{\mathscr{H}^{1/2}}{\sigma_p \gamma^3 \sqrt{\beta_y}}\right) \ , \tag{8-12}$$

where $C = 10^{-9}\ m^2/(A\text{-sec})$ for $\varepsilon_y = \varepsilon_x/10$. [Note: Equation (8-12) is intended only to show some characteristic behavior on beam and lattice parameters; evaluation of the full theoretical analysis is required for design specification.] Thus, large I_p and $\mathscr{H}$ (dispersion), small emittances ε_x and σ_p, and high vertical density (small $\sqrt{\beta_y}$) tend to increase the diffusion rate. Typically, $\varepsilon_x = 10^{-8}$m-rad yields diffusion rates of tens of milliseconds at an energy of 500 MeV and currents of a few hundred amperes.

The equilibrium emittance ε is a "sum" of the quantum excitation natural emittance and the multiple intrabeam scattering diffusion. Again, for typical cases, ε is found to satisfy the relationship

$$\varepsilon = \frac{1}{2}\left[\varepsilon_0 + \sqrt{\varepsilon_0^2 + C\left(\frac{I_p \mathscr{H}^{1/2}}{\sigma_p \gamma^3 \sqrt{\beta_y} g}\right)}\right] , \tag{8-13}$$

where ε_0 is the natural emittance and g is the horizontal emittance damping rate from synchrotron radiation.

As discussed earlier, single, large-angle scattering can limit the beam lifetime by causing particle momenta to exceed the bucket height or dynamic aperture of the storage ring. At 500 MeV, peak currents of a hundred amperes and a horizontal emittance at the 10^{-8}m-rad level appear to demand a momentum aperture of 3% for lifetimes of about one hour. Dynamic apertures below 2% give intolerably short lifetimes at these high peak currents.

8.3 Lattice Optimization

The basic goal of the lattice design is to maximize I_p/ϵ_x. Combining the results of the previous sections, we have

$$\frac{I_p}{\epsilon_x} = \frac{\frac{2\pi\alpha(\frac{E}{e})\sigma_p^2}{(Z/n)}}{1/2\left[\epsilon_o + \sqrt{\epsilon_o^2 + C\left(\frac{2\pi\alpha(\frac{E}{e})\sigma_p^2}{(Z/n)}\right)\left(\frac{\mathcal{H}^{1/2}}{\sigma_p\gamma^3\sqrt{\beta_y}g}\right)}\right]} \quad . \tag{8-14}$$

Although this relationship is self-explanatory, a few comments are in order. First, the benefits of increased damping (g) suggest the introduction of damping wigglers with the bonus of diminishing the natural emittance ϵ_o. For smaller rings, this improvement may be partially cancelled by the introduction of an additional free-space impedance resulting from synchrotron radiation:

$$(Z/n)_{wigglers} = 300\,\frac{h}{R}\,\frac{(\Delta\theta)}{2\pi}\ , \tag{8-15}$$

where $\Delta\theta$ is the total absolute-value bend of the wiggler. Second, when the denominator is dominated by the intrabeam scattering term, then

$$\frac{I_p}{\epsilon} \propto \sqrt{\frac{\alpha}{\mathcal{H}^{1/2}}}\ . \tag{8-16}$$

In the smooth approximation, $\mathcal{H}^{1/2}$ and α are proportional and the dependence on α vanishes. Somewhat more physically, large α allows higher peak current by increasing the microwave instability threshold. This higher peak current, however, increases the intrabeam scattering diffusion. Moreover, the larger dispersion associated with increasing the momentum compaction α enhances betatron excitation. The lesson here is to pursue lattice designs that decouple α and $\mathcal{H}$ as much as possible. Finally, lattices with larger β_y (i.e., lower vertical electron density) in dispersive regions are to be preferred.

The basic goal remains optimization of the FEL gain parameter ρ. As indicated in this section, some preliminary storage-ring studies imply that currents of several hundred amperes are consistent with horizontal emittance ϵ_x and longitudinal σ_p at the 10^{-8}m-rad and 10^{-3} level, respectively, at low energies (500 MeV). For typical undulator designs, these storage-ring parameters yield a ρ of about 10^{-3}. In light of inequality (Eq. 8-4), this result is encouraging.

8.4 References

8-1. K-J. Kim, J.J. Bisognano, A.A. Garren, and J.M. Peterson, "Issues in Storage Ring Design for Operation of High Gain FEL," Proceedings of Workshop on Coherent and Collective Propagation of Relativistic Electron Beams and Electromagnetic Radiation, Villa Olmo, Como, Italy (Sept. 1984).

8-2. For a review, see J.L. Laclare, XIth Intl. Conf. High Energy Acc., Geneva (1980) p. 526.

8-3. A.W. Chao and J. Gareyte, pep-224 (1976).

8-4. A. Faltens and L.J. Laslett, Isabelle Summer Study, BNL-20550 (1975) 486.

8-5. A. Piwinski, "Intra-beam Scattering," XIth Int. Conf. High Energy Acc., SLAC (1974).

8-6. J. Bjorken and S. Mtingwa, Particle Acc. 13, 115 (1983).

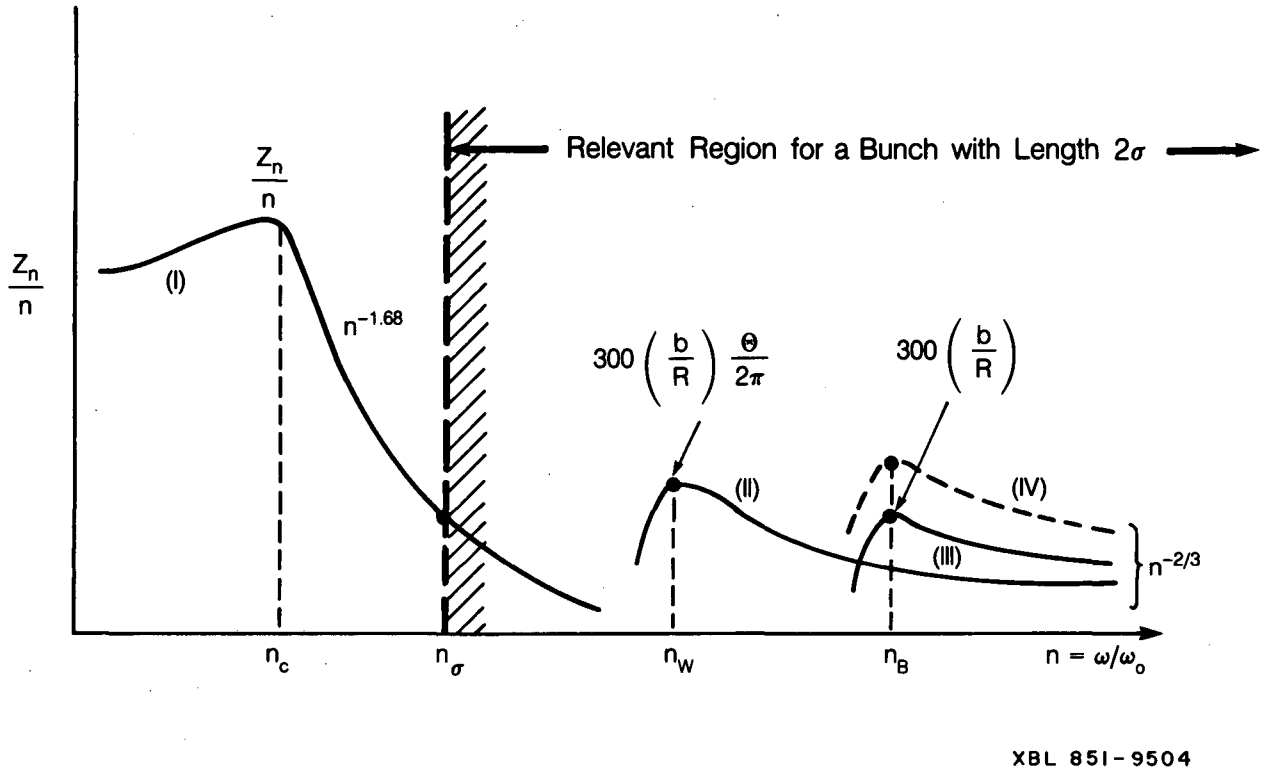

Figure 8-1. Qualitative behavior of typical broadband impedance. Here $n_C = R/b$, $n_\sigma = R/\sigma_S$, $n_{W,B} = R(\pi\rho_{W,B}/2b)^{3/2}/\rho_{W,B}$.

LAWRENCE BERKELEY LABORATORY
TECHNICAL INFORMATION DEPARTMENT
UNIVERSITY OF CALIFORNIA
BERKELEY, CALIFORNIA 94720